Soft-Tissue Sarcomas of the Abdomen and Pelvis: Radiologic-Pathologic Features, Part 1—Common Sarcomas[1]

Angela D. Levy, MD
Maria A. Manning, MD
Waddah B. Al-Refaie, MD
Markku M. Miettinen, MD

Abbreviations: GIST = gastrointestinal stromal tumor, H-E = hematoxylin-eosin, IVC = inferior vena cava, WHO = World Health Organization

RadioGraphics 2017; 37:462–483

Published online 10.1148/rg.2017160157

Content Codes: CT GI MR OI

[1]From the Departments of Radiology (A.D.L., M.A.M.) and Surgery (W.B.A.), Medstar Georgetown University Hospital, 3800 Reservoir Rd NW, Washington, DC 20007; the American Institute for Radiologic Pathology, Silver Spring, Md (M.A.M.); and the Center for Cancer Research, National Cancer Institute, Bethesda, Md (M.M.M.). Received June 14, 2016; revision requested August 8 and received September 28; accepted October 11. For this journal-based SA-CME activity, the authors, editor, and reviewers have disclosed no relevant relationships. **Address correspondence to** A.D.L. (e-mail: *angela.d.levy@gunet.georgetown.edu*).

Supported by the American Institute for Radiologic Pathology, the Joint Pathology Center, and the Uniformed Services University of the Health Sciences. The views expressed in this article are those of the authors and do not necessarily reflect the official policy or position of the Department of Defense or the U.S. Government.

SA-CME LEARNING OBJECTIVES

After completing this journal-based SA-CME activity, participants will be able to:

- Discuss the classification of soft-tissue sarcomas.
- Describe and illustrate the radiologic and pathologic features of liposarcoma, leiomyosarcoma, and GIST, which are the most common soft-tissue sarcomas of the abdomen and pelvis.
- Identify the imaging findings that are most important for preoperative characterization and anatomic localization of soft-tissue sarcomas in the abdomen and pelvis.

See www.rsna.org/education/search/RG.

Soft-tissue sarcomas are a diverse group of rare mesenchymal malignancies that can arise at any location in the body and affect all age groups. These sarcomas are most common in the extremities, trunk wall, retroperitoneum, and head and neck. In the adult population, soft-tissue sarcomas arising in the abdomen and pelvis are often large masses at the time of diagnosis because they are usually clinically silent or cause vague or mild symptoms until they invade or compress vital organs. In contrast, soft-tissue sarcomas arising from the abdominal wall come to clinical attention earlier in the course of disease because they cause a palpable mass, abdominal wall deformity, or pain that is more clinically apparent. The imaging features of abdominal and pelvic sarcomas and abdominal wall sarcomas can be nonspecific and overlap with more common pathologic conditions, making diagnosis difficult or, in some cases, delaying diagnosis. Liposarcoma (well-differentiated and dedifferentiated liposarcomas), leiomyosarcoma, and gastrointestinal stromal tumor (GIST) are the most common intra-abdominal primary sarcomas. Any soft-tissue sarcoma can arise in the abdominal wall. Knowledge of the classification and pathologic features of soft-tissue sarcomas, the anatomic locations where they occur, and their cross-sectional imaging features helps the radiologist establish the diagnosis or differential diagnosis so that patients with soft-tissue sarcomas can receive optimal treatment and management. In part 1 of this article, the most common soft-tissue sarcomas (liposarcoma, leiomyosarcoma, and GIST) are reviewed, with a discussion on anatomic locations, classification, clinical considerations, and differential diagnosis. Part 2 will focus on the remainder of the soft-tissue sarcomas occurring in the abdomen and pelvis.

Introduction

Sarcomas are a large, diverse group of malignant tumors of mesenchymal origin. The World Health Organization (WHO) divides sarcomas into two broad categories: sarcomas of soft tissue and sarcomas of bone (1). Soft-tissue sarcomas affect all ages and may arise at any location in the body. They account for less than 1% of malignant tumors. The estimated number of new soft-tissue sarcomas in the United States in 2016 is 12 310 cases, and the number of estimated deaths is 4990 (2). Approximately 60% of soft-tissue sarcomas originate in an extremity (most commonly, the thigh), 19% in the trunk wall, 15% in the retroperitoneum, and 9% in the head and neck (3).

Liposarcoma (specifically, well-differentiated and dedifferentiated liposarcomas) and leiomyosarcoma are the most common intra-abdominal soft-tissue sarcomas, and the retroperitoneum is their most common location. Gastrointestinal stromal tumor (GIST) is the most common gastrointestinal and intraperitoneal sarcoma. GIST is included in this discussion because of its inclusion in the 2013 WHO

TEACHING POINTS

- Liposarcoma (specifically, well-differentiated and dedifferentiated liposarcomas) and leiomyosarcoma are the most common intra-abdominal soft-tissue sarcomas, and the retroperitoneum is their most common location.
- Well-differentiated retroperitoneal liposarcoma may contain thin or irregular septa, minor nodular soft-tissue components, and thin blood vessels.
- Leiomyosarcomas arising from the IVC and major veins of the retroperitoneum and pelvis may manifest as an intraluminal mass, an extraluminal mass, or both.
- Malignant GISTs are the most common intraperitoneal sarcomas, and these tumors also occur in the retroperitoneum, given the retroperitoneal location of parts of the gastrointestinal tract.
- The key to the imaging diagnosis of a GIST is establishing its origin from the wall of the stomach or intestine, although rare cases can appear to be extragastrointestinal.

classification of soft-tissue sarcomas; this inclusion was one of the most important changes in the updated WHO classification (Table 1) (1,4). GIST is also an important tumor for radiologists to recognize and differentiate from other intra-abdominal and gastrointestinal malignancies because of its unique clinical management.

The presenting clinical manifestations and often the imaging findings of soft-tissue sarcomas are nonspecific. The typical scenario is the discovery of a large abdominal or pelvic mass in a patient who is imaged for abdominal fullness or pain. The differential diagnosis will depend primarily on the anatomic location. Soft-tissue sarcomas arising in the abdomen and pelvis may occur in all anatomic compartments, the retroperitoneum, peritoneal cavity, and abdominal wall. However, knowledge of the imaging and pathologic features of soft-tissue sarcomas is important in the differential diagnosis. Because soft-tissue sarcomas are rare and can be difficult to treat and manage, an accurate initial diagnosis is essential for these patients. In this article, the clinical-pathologic and radiologic features of the most common abdominal and pelvic sarcomas in adults are reviewed. An emphasis is placed on establishing an appropriate differential diagnosis on the basis of the anatomic location and radiologic features. Sarcomas arising in solid visceral organs, such as the liver, spleen, and uterus, are not discussed in this article.

Anatomic Considerations

The retroperitoneum and trunk wall are the most common locations for soft-tissue sarcomas of the abdomen and pelvis. Less commonly, soft-tissue sarcomas originate in the peritoneal cavity and extraperitoneal pelvis. A thorough understanding of the anatomy of the retroperitoneum, peritoneal

Table 1: Classification of Soft-Tissue Sarcomas Occurring in the Abdomen and Pelvis on the Basis of the 2013 WHO Classification of Tumors of Soft Tissue

Categories of Soft-Tissue Tumors, with the Sarcomas Classified in Each Category
Adipocytic tumors
Well-differentiated liposarcoma
Dedifferentiated liposarcoma
Pleomorphic liposarcoma
Myxoid liposarcoma
Fibroblastic/myofibroblastic tumors
Dermatofibrosarcoma protuberans
Solitary fibrous tumor
Fibrosarcoma
Myxoid fibrosarcoma
So-called fibrohistiocytic tumors
Malignant tenosynovial giant cell tumor
Smooth muscle tumors
Leiomyosarcoma
Pericytic (perivascular) tumors
Malignant glomus tumor
Skeletal muscle tumors
Embryonal rhabdomyosarcoma
Alveolar rhabdomyosarcoma
Pleomorphic rhabdomyosarcoma
Spindle cell/sclerosing rhabdomyosarcoma
Vascular tumors of soft tissue
Epithelioid hemangioendothelioma
Angiosarcoma
Chondro-osseous tumors
Extraskeletal osteosarcoma
GISTs
Malignant GISTs
Nerve sheath tumors
Malignant peripheral nerve sheath tumor
Ectomesenchymoma
Tumors of uncertain differentiation
Synovial sarcoma
Epithelioid sarcoma
Alveolar soft part sarcoma
Clear cell sarcoma of soft tissue
Extraskeletal myxoid chondrosarcoma
Extraskeletal Ewing sarcoma
Desmoplastic small round cell tumor
Extrarenal rhabdoid tumor
Perivascular epithelioid cell tumor (PEComa)
Undifferentiated/unclassified sarcomas
Undifferentiated pleomorphic sarcoma (previously called malignant fibrous histiocytoma)
Undifferentiated spindle cell sarcoma
Undifferentiated round cell sarcoma
Undifferentiated epithelioid sarcoma

cavity, extraperitoneal pelvis, and abdominal wall is necessary to establish a working differential diagnosis and to assist in preoperative planning.

The retroperitoneum is located posterior to the peritoneal cavity, extending from the diaphragm superiorly to the pelvic brim inferiorly. The posterior parietal peritoneum is the anterior boundary, and the transversalis fascia is the posterior boundary. The fascial planes within the retroperitoneum form three distinct compartments: the anterior pararenal space, perirenal space, and posterior pararenal space (Fig 1). When a mass is discovered in the retroperitoneum, soft-tissue sarcoma should be considered at the top of the differential diagnosis when the mass cannot be shown to originate from a visceral organ contained within the retroperitoneum.

In the retroperitoneum, the anterior pararenal space is bounded anteriorly by the posterior parietal peritoneum and posteriorly by the Gerota fascia and is contiguous across the midline. The pancreas, duodenum, and ascending and descending colon are located within the anterior pararenal space (Fig 1).

The perirenal space contains the adrenal glands and kidneys. Anteriorly, the perirenal space is bounded by the Gerota fascia and posteriorly by the Zuckerkandl fascia (5,6). The lateral boundaries of the anterior pararenal and perirenal spaces are formed by the fusion of the Gerota and Zuckerkandl fasciae, which is called the lateral conal fascia (7). The lateral conal fascia extends anterolaterally to merge with the parietal peritoneum. At computed tomography (CT), these fascial boundaries are thin, barely perceptible soft-tissue lines in normal patients. Medially, the renal fascia fuses onto the great vessels, creating a separation between the right and left perirenal spaces. However, in some individuals, communication between the two perirenal spaces has been observed at CT, supporting an argument that there is midline continuity of the perirenal space and anatomic variability from person to person (8,9). Superiorly, the perirenal space is closed by the fusion of the Gerota and Zuckerkandl fasciae with each other and the diaphragm (Fig 2a). Inferiorly, controversy continues to exist about whether there is fusion between the perirenal fascial layers, resulting in caudal closure of the perirenal space, or if this space remains open because of blending of the fascia with adjacent adipose tissue (10). Nevertheless, retroperitoneal sarcomas may grow longitudinally within the retroperitoneum to extend cranially toward the diaphragm and caudally into the pelvis.

The posterior pararenal space contains only fat. It is bounded anteriorly by the Zuckerkandl fascia and the lateral conal fascia and posteriorly by the transversalis fascia. The quadratus lumborum and psoas muscles form the medial border. Laterally, the posterior pararenal space communicates with the properitoneal fat (7).

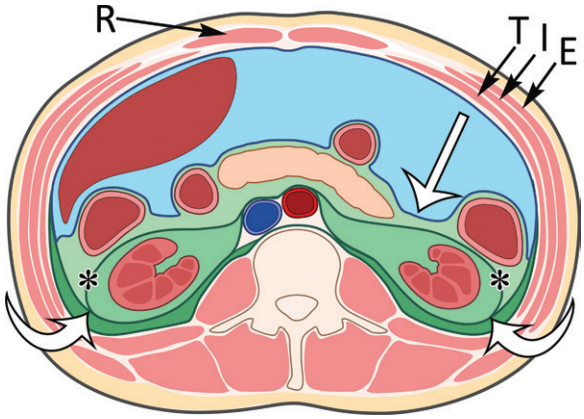

Figure 1. Compartments within the retroperitoneum as defined by fascial planes. Drawing of the abdominal compartments in the axial plane shows the peritoneal cavity (blue) separated from the retroperitoneum (various shades of green) by the posterior parietal peritoneum (straight white arrow). The retroperitoneal compartments include the anterior pararenal space (light green), the perirenal space (medium green) bounded by the Gerota fascia (*), and the posterior pararenal space (dark green). The fusion of the Gerota and Zuckerkandl fasciae forms the lateral conal fascia (curved white arrows), which separates the lateral anterior pararenal space from the posterior pararenal space. In the anterior abdominal wall, the rectus abdominis muscles *(R)* are in the midline and contained in the rectus sheath. The external oblique *(E)*, internal oblique *(I)*, and transverse abdominis *(T)* muscles form the muscular layers of the anterolateral abdominal wall.

Within the abdomen and pelvis, the peritoneal cavity is anteriorly located and contained by its serosal membrane, the peritoneum (Fig 2b). The peritoneum is divided into parietal and visceral components. The parietal peritoneum lines the anterior, lateral, and posterior abdominal walls; the undersurface of the diaphragm; the anterior surface of the retroperitoneal viscera; and the pelvis. The visceral peritoneum covers the intraperitoneal organs, omenta, and mesenteries.

The extraperitoneal pelvis is that portion of the pelvis that is separated from the peritoneal cavity by parietal peritoneum, which covers the pelvic organs (Fig 2b). Although the extraperitoneal pelvis is distinctly separate from the peritoneal cavity, aggressive sarcomas frequently cross this anatomic plane.

The abdominal wall is formed from superficial to deep by the skin, subcutaneous fat, fascia, and muscles. The muscular layer of the abdominal wall is separated from the peritoneum by the transversalis fascia and properitoneal fat. Laterally, the muscles of the abdominal wall, from outer to inner, are the external oblique, internal oblique, and transversus abdominis (Fig 1). The anterior extension of the aponeurosis of these muscles forms

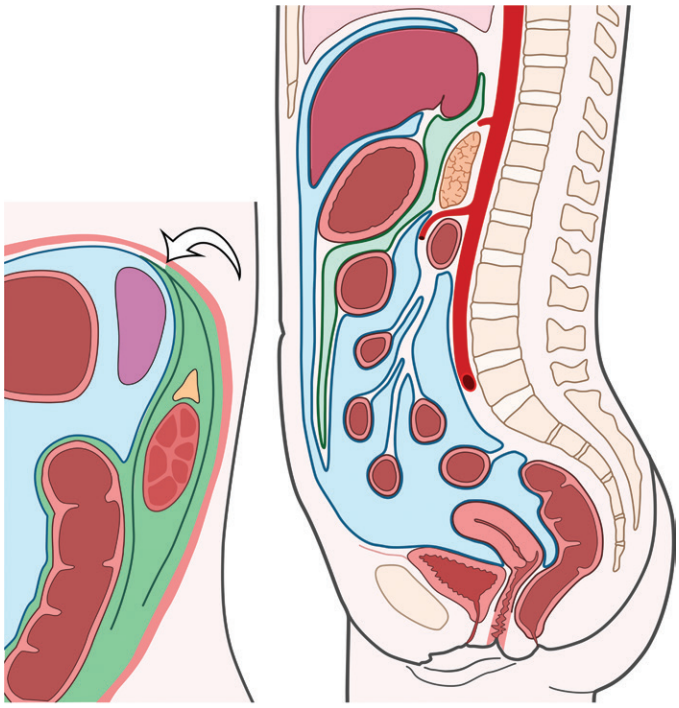

Figure 2. Fascial planes of the abdomen and pelvis. **(a)** Drawing of the retroperitoneum (green) in the sagittal plane shows the superior boundary formed by fusion of the posterior parietal peritoneum, Gerota fascia, and Zuckerkandl fascia with the undersurface of the diaphragm (arrow). **(b)** Drawing of the abdomen and pelvis in the sagittal plane shows the peritoneal cavity (blue) distinct from the retroperitoneal and extraperitoneal spaces.

the rectus sheath. Its lateral boundary is the linea semilunaris, from which it extends anteriorly to contain the rectus abdominis muscles, which are the muscles of the anterior abdominal wall. They are sandwiched between the anterior and posterior laminae of the rectus sheath. These laminae fuse in the midline of the anterior abdominal wall to form the linea alba. The muscles of the posterior abdominal wall are the latissimus dorsi, quadratus lumborum, and the paraspinal muscles. Soft-tissue sarcomas of the abdominal wall primarily arise within the musculature, with the exception of dermatofibrosarcoma protuberans, which arises superficially in the dermis.

Soft-Tissue Sarcoma Classification, Grading, and Staging

The WHO classification is the accepted standardization of nomenclature and classification for soft-tissue sarcomas (Table 1) (1). The names of the sarcomas are derived from the cell type they resemble histologically and immunohistochemically. The purpose of classification is to create a framework for treatment and management of patients with soft-tissue sarcomas that is based on tumor biology. However, the biologic behavior of the majority of soft-tissue sarcomas cannot be predicted by tissue type alone. Tumor grading and staging strongly correlate with prognosis. Tumor grade is an estimate of the degree of malignancy. The grading system set forth by the French Federation of Cancer Centers is the most widely used (11). Histologic tumor grade is determined by a scoring system that assesses tumor differentiation, mitotic count, and tumor necrosis.

Tumor staging is achieved with a combination radiologic, surgical, and histologic grade. The American Joint Committee on Cancer (AJCC) staging system for soft-tissue sarcoma is the most widely used for abdominal and pelvic sarcomas (12). The AJCC staging system for sarcomas combines the size of the primary tumor (T), the involvement of lymph nodes (N), the presence of metastasis (M), the type and grade of sarcoma (G), and tumor depth. The AJCC staging system can be applied to sarcomas at any anatomic site and, as such, is useful for sarcomas arising in the abdomen and pelvis (13). The other commonly used staging system is the Musculoskeletal Tumor Society system, which is based on anatomic compartmentalization and is therefore most useful for sarcomas in the extremities (14,15).

Radiologic Evaluation of Abdominal and Pelvic Soft-Tissue Sarcomas

Radiologic characterization and staging of abdominal and pelvic soft-tissue sarcomas are best achieved with the cross-sectional imaging modalities that provide excellent tissue characterization and anatomic visualization. CT is the most widely used cross-sectional imaging modality for the abdomen and pelvis because of its wide availability, ease of use, and capability to image the breadth of anatomy (chest, abdomen, and pelvis) simultaneously for staging. CT can be used to effectively characterize tissue components, which is necessary

to establish a working differential diagnosis, and CT offers multiplanar reconstructions to easily depict the anatomic site of origin of a mass, as well as its relationship to adjacent organs and vasculature. Magnetic resonance (MR) imaging is an excellent complement to CT for tissue characterization because MR imaging has superior contrast resolution. MR imaging may help in assessing local invasion for staging, but MR imaging is less practical for overall staging because it is more difficult to image the entire body with MR imaging, compared with CT. Combined imaging with positron emission tomography and CT is useful for identifying unsuspected distant metastases and for problem solving of indeterminate findings seen on CT or MR images during initial staging and restaging in patients after neoadjuvant therapy or resection.

Ultrasonography (US) may be used as an initial imaging modality during the evaluation of patients with abdominal complaints or palpable abdominal wall masses. However, US is less useful for evaluating the entire abdomen and pelvis for preoperative planning and surveillance imaging because US has a limited depth of penetration to evaluate deep abdominal structures such as the bowel and their relationship to the mass. US is useful for directing imaging-guided biopsies. Finally, unlike sarcomas of the extremities, abdominal radiography is not useful for intra-abdominal and abdominal wall sarcomas because of inadequate soft-tissue differentiation and an inability to locate the abdominal mass and define its relationship to abdominal organs. In this review, the CT and MR imaging manifestations of soft-tissue sarcomas are discussed.

Most Common Sarcomas of the Abdomen and Pelvis

Liposarcoma

Definition.—*Liposarcoma* is the term for a malignant tumor that has fatty differentiation. The tumors that make up this group (well-differentiated, dedifferentiated, pleomorphic, and myxoid liposarcomas) are distinctly different histologically and genetically, and they vary in biologic behavior.

Clinical and Pathologic Features.—Liposarcoma is the most common sarcoma in adults and the most commonly occurring sarcoma in the retroperitoneum (16). Well-differentiated liposarcoma, which is synonymously called atypical lipomatous tumor (especially when located outside body cavities), is the most common type of liposarcoma in the retroperitoneum. This tumor does not metastasize, but it may progress into a nonlipomatous form referred to as dedifferentiated liposarcoma and then obtain the capability to metastasize. Pleomorphic liposarcoma is extremely rare in the retroperitoneum. Myxoid liposarcoma does not usually occur as a primary tumor in the retroperitoneum but can metastasize there from a primary tumor in a lower extremity.

Clinical symptoms of abdominal and pelvic sarcomas are most often related to tumor size. Because most liposarcomas occur in the retroperitoneum, they are clinically silent until they grow to large sizes. They may be more than 20 cm in largest diameter at the time of diagnosis (17). Pain, symptoms of mass effect, organ compression, or physical deformity of the abdominal cavity bring patients to clinical attention. Occasionally, liposarcoma may be discovered when a patient is imaged with CT or MR imaging for unrelated abdominal symptoms or for vague or nonspecific symptoms.

Well-differentiated liposarcoma, or atypical lipomatous tumor, is the most common histologic type of liposarcoma, representing more than 40%–45% of all liposarcomas. It occurs in middle-aged and older adults, with a peak incidence in the 6th decade of life (18). At gross pathologic examination, well-differentiated liposarcoma of the retroperitoneum is typically a large multinodular tumor. The cut surface varies from fatlike pale yellow to white or gray in color, and it can have a mucoid appearance. Fibrous septa and sclerosing components may be seen throughout the mass. Histologically, nuclear atypia in adipocytes or septal cells distinguishes well-differentiated liposarcoma from lipoma. Variation in cell size, areas of fat necrosis, and lymphoid infiltration are also distinguishing features (19).

The WHO defines three distinct histologic patterns in well-differentiated liposarcoma: lipoma-like, sclerosing, and inflammatory (1). Each pattern may be the predominant histology in a particular tumor or may overlap and coexist with the other patterns in the same tumor. The lipoma-like pattern resembles a benign lipoma, but the adipocytes vary in size and demonstrate variable atypia. There may also be septal hypercellularity with nuclear atypia (20). The lipoma-like pattern may be mistaken for a benign lipoma when small biopsy specimens are obtained or when the tumor is undersampled. The sclerosing variant most commonly occurs in the retroperitoneum and paratesticular region. The majority of the lesion is characterized by the presence of atypical cells in a dense collagenous stroma (21). Myxoid and lipogenic areas may also be present. The inflammatory variant contains lymphoid aggregates in addition to the previously listed features.

Dedifferentiated liposarcoma can be understood as a progression or variant of well-differentiated liposarcoma. This variant is relatively

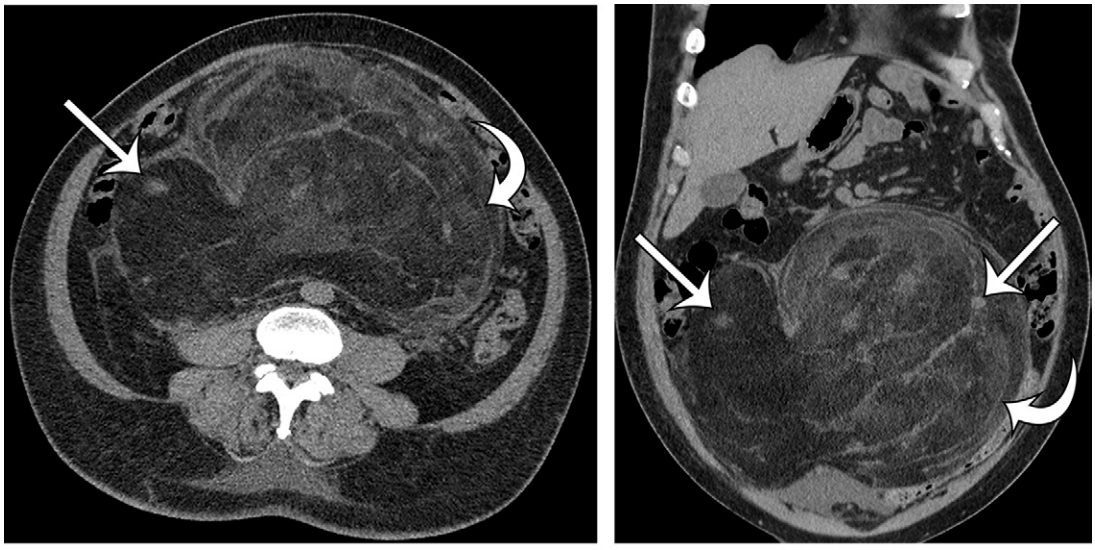

a. b.

Figure 3. Well-differentiated liposarcoma in a 67-year-old man who complained of abdominal distention and pain. Axial **(a)** and coronal **(b)** nonenhanced CT images show a large well-defined, predominantly fat-attenuation mass, with thin septa (curved arrow) and small soft-tissue nodules (straight arrows).

uncommon and can occur without a preceding well-differentiated liposarcoma or as a component of a well-differentiated liposarcoma (22). Dedifferentiated liposarcoma with low-grade features is relatively indolent, and high-grade tumors often metastasize. In all, distant metastases arise in up to 18% of patients (22,23). At gross pathologic examination, dedifferentiated liposarcoma is a firm white or yellow solid nonlipogenic mass. Histologically, low-grade dedifferentiated tumors are usually composed of spindle-shaped cells with nuclear atypia, whereas high-grade dedifferentiated liposarcoma resembles undifferentiated pleomorphic sarcoma or myxofibrosarcoma (22). There is often a sharp demarcation between the well-differentiated and dedifferentiated components.

Myxoid liposarcoma is the second most common liposarcoma (30%–40%). It occurs almost exclusively in the extremities in a young adult patient population (median age, 44 years) (24,25). Myxoid liposarcoma is extremely rare in the retroperitoneum and is usually metastatic in this location. It is a soft gelatinous tumor at gross pathologic examination. Histologically, there are ovoid to round cells around prominent capillaries in a myxoid stroma. Cells of fatty differentiation may be interspersed in the tumor (26). Myxoid features in well-differentiated liposarcoma should not be confused with myxoid liposarcoma.

Pleomorphic liposarcoma is the rarest type of liposarcoma, accounting for less than 5% of cases (27). It occurs in older adults (peak incidence in the 7th decade), with a male predominance (28). The retroperitoneum and trunk wall are uncommon sites because a majority of these tumors arise in the extremities. At gross pathologic examination, pleomorphic liposarcomas are often firm yellow tumors. Histologically, they often contain abundant pleomorphic lipoblasts, but they can also resemble undifferentiated pleomorphic sarcoma or can have an epithelioid appearance resembling adrenal or renal carcinoma (28).

Radiologic Features.—Well-differentiated liposarcoma is a well-defined mass demonstrating fat attenuation at CT (Fig 3). At MR imaging, the signal intensity of the fat in well-differentiated liposarcoma resembles the signal intensity of the subcutaneous fat (29). Well-differentiated liposarcoma has high signal intensity on T1- and T2-weighted MR images and loses signal intensity on fat-suppressed MR images (Fig 4). Well-differentiated liposarcoma is generally round, oval, or lobulated and exerts mass effect on adjacent normal anatomic structures. It may compress, displace, and distort adjacent anatomic structures. In the retroperitoneum, well-differentiated liposarcoma frequently grows longitudinally, such that it extends the entire cranial-to-caudal length of the retroperitoneum while also growing centripetally. Similar to an atypical lipomatous tumor in the extremity, well-differentiated retroperitoneal liposarcoma may contain thin or irregular septa, minor nodular soft-tissue components, and thin blood vessels (Fig 3) (30). The septa may enhance after administration of intravenous contrast material, but in general, well-differentiated retroperitoneal liposarcoma is a poorly vascularized lesion with little or no enhancement. Myxoid components of well-differentiated liposarcoma demonstrate water

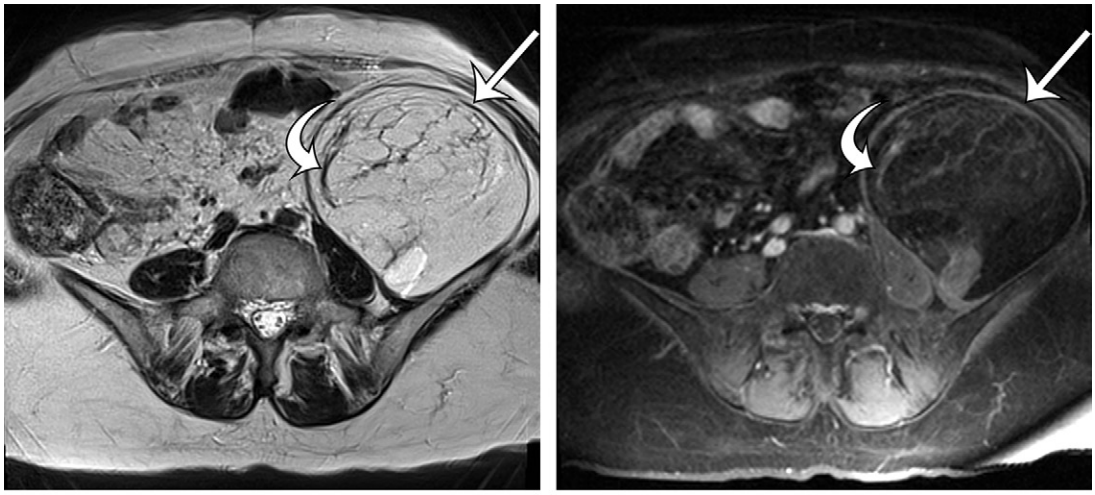

a. b.

c.

Figure 4. MR imaging features of well-differentiated liposarcoma in a 74-year-old woman with worsening back pain. **(a)** Axial T2-weighted MR image shows a well-defined high-signal-intensity mass (straight arrow) in the left retroperitoneum; the mass has internal septa (curved arrow). **(b)** Axial contrast material–enhanced T1-weighted fat-suppressed MR image shows that the mass (straight arrow) demonstrates a loss of signal intensity, with signal intensity similar to that of the subcutaneous fat. The thin septa (curved arrow) are enhanced. **(c)** Sagittal T2-weighted MR image shows longitudinal growth of the mass in the retroperitoneum, with well-defined margins (arrows) between the mass and the retroperitoneal fat superiorly.

attenuation on CT images, low signal intensity on T1-weighted MR images, and high signal intensity on T2-weighted MR images. Typically, enhancement after intravenous contrast material administration in myxoid components can be difficult to appreciate on CT images. However, gradual reticular enhancement within myxoid regions can be seen at MR imaging (31). MR imaging subtraction techniques can be used to improve depiction of enhancing components. The sclerosing variant of well-differentiated liposarcoma is usually well circumscribed but may have infiltrative margins (Fig 5) (32). The sclerosing variant may have a paucity of fat, such that it mimics high-grade liposarcomas such as dedifferentiated or pleomorphic liposarcomas (31,32). The nonfatty component demonstrates soft-tissue attenuation on CT images and has a variable degree of high signal intensity on T2-weighted MR images.

Dedifferentiated liposarcomas are heterogeneous solid soft-tissue masses on CT and MR images (Fig 6). Because these tumors frequently contain regions of variable histologic findings, well-defined fat and myxoid areas may be seen within a single tumor (33). Classically, a sharp demarcation between fatty and nonfatty elements is characteristic on CT or MR images, a finding that parallels the sharp demarcation between well-differentiated and dedifferentiated components that is observed histologically. However, a more blended or gradual transition between these components has also been described (25,33). In some cases, the fat component predominates, which is suggestive of dedifferentiation within a well-differentiated liposarcoma. Calcification and ossification may be present, correlating with metaplasia or osteochondromatous or chondrosarcomatous components of the tumor (33,34).

Myxoid liposarcoma contains an abundant myxoid matrix with a high water content that is hypoattenuating on CT images, hypointense on T1-weighted MR images, and hyperintense on T2-weighted MR images. It is important to demonstrate enhancement of the myxoid matrix to distinguish it from a cystic mass. Enhancement may not be appreciated on CT images but can be well seen on MR images. Thick enhancing septa characteristically course through the mass, as well as an enhancing patchy or nodular soft-tissue component that demonstrates intermediate signal intensity on T1- and T2-weighted MR images (29). The septa correspond to fibrous

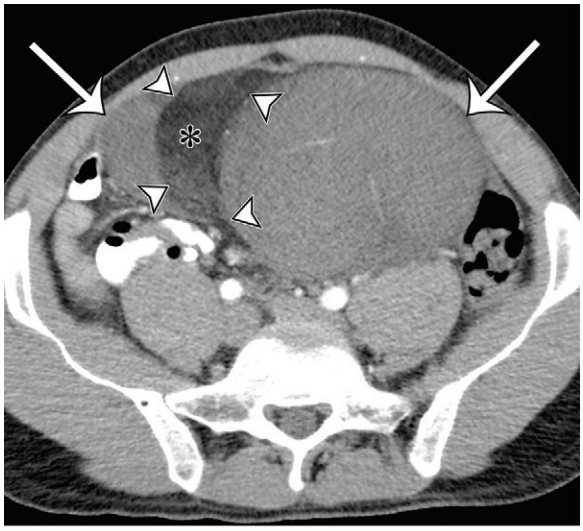

a.

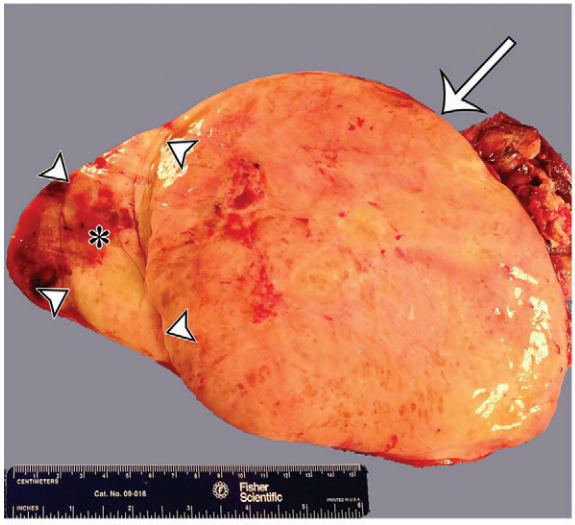

b.

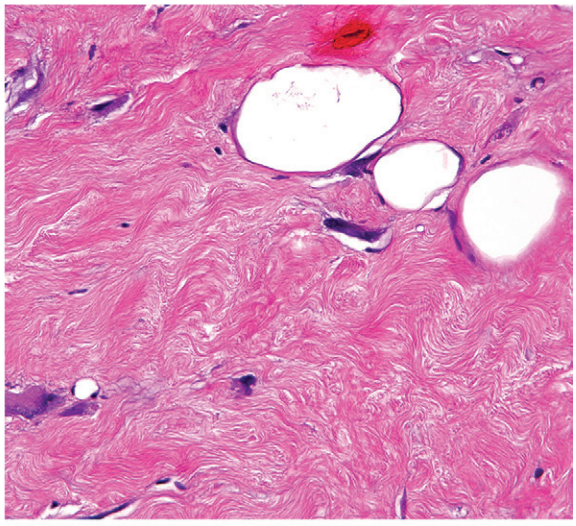

c.

Figure 5. Sclerosing type of well-differentiated liposarcoma in a 37-year-old man with severe abdominal pain. **(a)** Axial contrast-enhanced CT image shows a large multinodular tumor with a fat-attenuation component (*) separated from the soft-tissue enhancing components (arrows) by thin septa (arrowheads). **(b)** Photograph of the cut surface of the gross specimen shows a similar configuration, with pale-yellow tissue correlating with the fat component (*) shown on **a**, and with pink-yellow tissue correlating with the soft-tissue components (arrow); the components are separated by fibrous septa (arrowheads). **(c)** Photomicrograph of the sclerosing type of well-differentiated liposarcoma shows a few adipocytes and nonlipomatous cells in a collagenous matrix. (Hematoxylin-eosin [H-E] stain; original magnification, ×40.)

bands coursing through the myxoid stroma. Foci of mature fat may be seen in the lesion.

Pleomorphic liposarcoma is a poorly defined soft-tissue mass with no distinguishing features on CT and MR images. Areas of low-attenuation heterogeneity on CT images represent degeneration, necrosis, or intratumoral hemorrhage. Fatty elements are not depicted on CT and MR images. Pleomorphic liposarcomas usually have no distinguishing features that allow them to be differentiated from leiomyosarcoma or undifferentiated pleomorphic sarcoma at imaging (29).

Recurrent and Metastatic Disease.—Recurrence of all types of retroperitoneal liposarcoma may follow initial surgical resection. Recurrences occur along the resection margins and at a distance from the initial resection bed. The imaging pattern (CT attenuation or MR imaging signal intensity) of the recurrent tumor is usually similar to the pattern that was seen in the initial mass (35). However, in well-differentiated liposarcoma, the recurrence can be a predominantly fatty mass or, in some cases, dedifferentiated liposarcoma without fat. When distant metastases occur, they most commonly arise in the lungs and liver (36).

Leiomyosarcoma

Definition.—Leiomyosarcomas are soft-tissue sarcomas with tumor cells resembling differentiated smooth muscle cells. The retroperitoneum is among the most common locations, and many of these tumors arise from the inferior vena cava (IVC) or other veins, such as renal, genital, or iliac veins (37).

Clinical and Pathologic Features.—Although leiomyosarcomas may occur at any age, middle-aged and older adults are the most commonly affected age groups, with substantial female predominance (37). Leiomyosarcoma is the second most common retroperitoneal sarcoma (after liposarcoma).

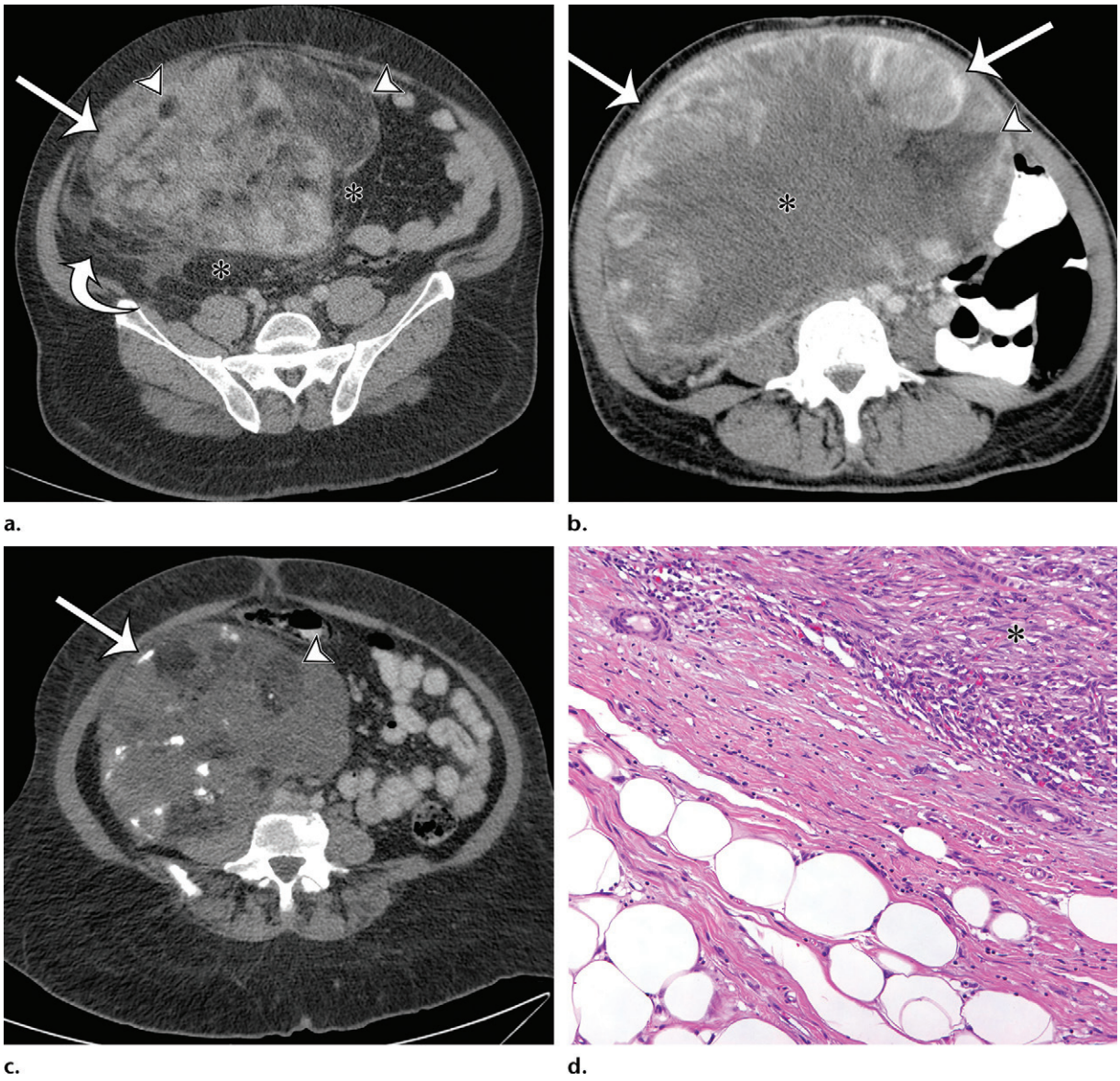

Figure 6. Spectrum of imaging appearances of dedifferentiated liposarcoma in three different patients. **(a)** Axial intravenous contrast material–enhanced CT image of dedifferentiated liposarcoma in a 58-year-old man shows areas of sharply demarcated fat (*) and blended fat (arrowheads), as well as larger enhancing solid components (straight arrow), with a less well-defined margin (curved arrow). **(b)** Axial intravenous and oral contrast material–enhanced CT image of dedifferentiated liposarcoma in a 72-year-old man shows progression to fewer areas of blended fat (arrowhead), with larger myxoid (*) and solid enhancing (arrows) components. **(c)** Axial intravenous and oral contrast material–enhanced CT image of dedifferentiated liposarcoma in a 68-year-old woman shows that in addition to blended fat (arrowhead) in a larger solid mass, coarse calcification (arrow) correlating with metaplasia or chondroosseous components can also be depicted. **(d)** Photomicrograph of dedifferentiated liposarcoma with well-differentiated components shows an abrupt transition between the nonlipogenic highly cellular dedifferentiated component (*) and the well-differentiated lipomatous component. (H-E stain; original magnification, ×40.)

Leiomyosarcomas may also rarely arise in the peritoneal cavity, the soft tissues of the pelvis, and the abdominal wall. In addition, metastatic leiomyosarcomas from uterine origin can involve the pelvis and other parts of the abdominal cavity.

The anatomic spaces of the retroperitoneum may allow leiomyosarcomas to grow to large sizes before causing clinical symptoms. Symptoms such as pain (back pain or radicular pain), abdominal distention, changes in bladder or bowel habits, and gastrointestinal bleeding are due to mass effect or organ involvement by the lesion. Leiomyosarcomas of the IVC may come to clinical attention earlier when they have an obstructive intravascular component or a large extraluminal component that causes venous compression, resulting in congestion of the lower extremities, kidneys, or liver. In these cases, Budd-Chiari syndrome or renal failure may be the initial clinical manifestation of the tumor (38).

At gross pathologic examination, leiomyosarcomas of low histologic grade resemble leiomyomas.

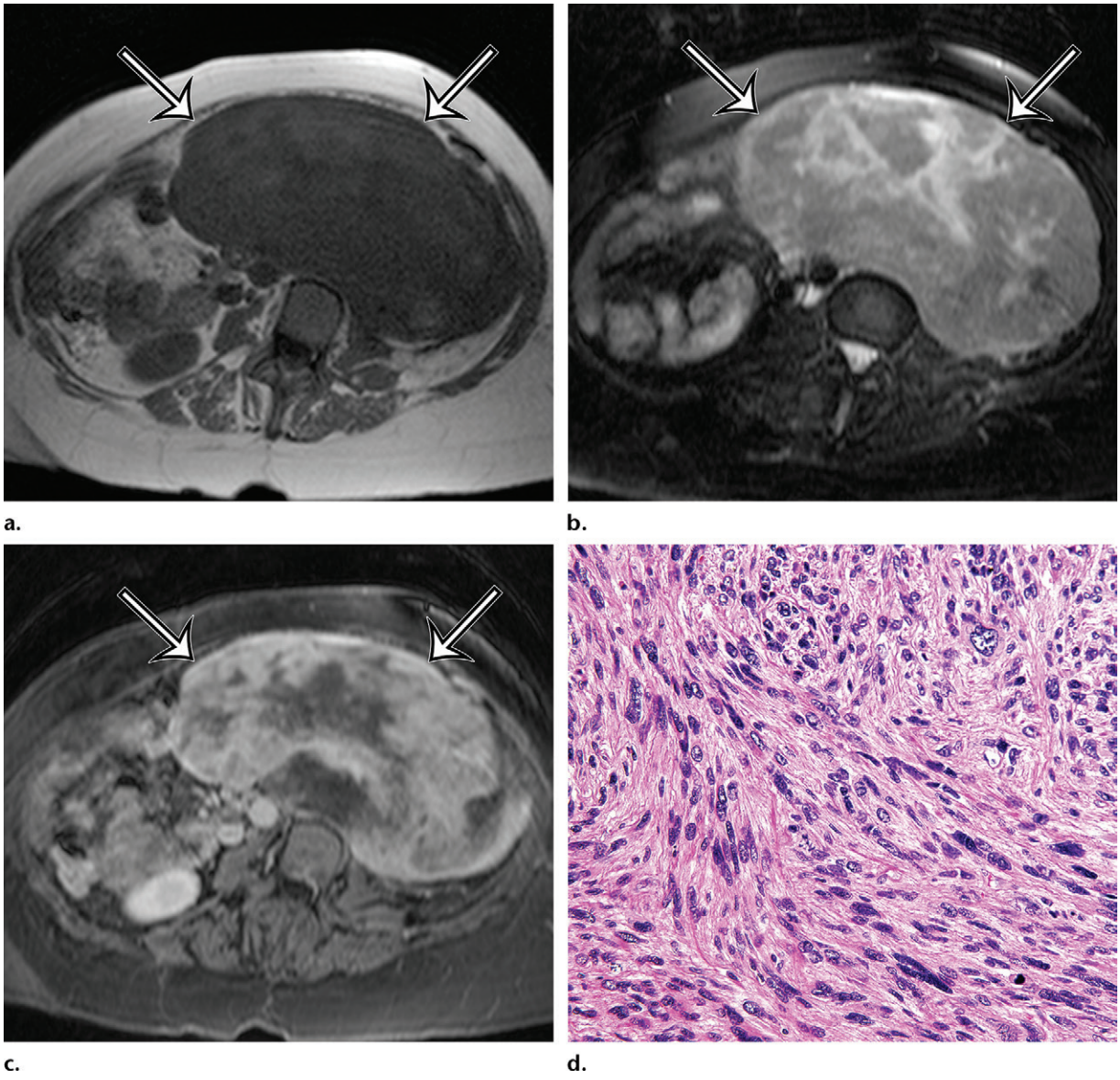

Figure 7. Incidentally identified intra-abdominal leiomyosarcoma in a 55-year-old woman. **(a–c)** Axial T1-weighted **(a)**, T2-weighted **(b)**, and gadolinium-enhanced T1-weighted fat-suppressed **(c)** MR images show a large relatively homogeneous, non–fat-containing solid intra-abdominal mass that is isointense to skeletal muscle on T1-weighted images (arrows on **a**), heterogeneously T2 hyperintense (arrows on **b**), and heterogeneously enhanced (arrows on **c**). **(d)** Photomicrograph of leiomyosarcoma shows elongated atypical spindle cells with blunt-ended nuclei with mitotic activity. (H-E stain; original magnification, ×80.)

They are a white or gray mass and may have a whorled appearance on the cut surface (37). High-grade tumors almost always have areas of hemorrhage and necrosis on their cut surface. Histologically, leiomyosarcomas are typically composed of elongated spindle cells with blunt-ended nuclei arranged in intersecting fascicles. Epithelioid cells or epithelioid cells admixed with spindle cells may be seen (39). High-grade tumors can demonstrate nuclear pleomorphism and may resemble other pleomorphic sarcomas (40).

Radiologic Features.—On CT images, retroperitoneal leiomyosarcomas are characteristically heterogeneous in attenuation because of the enhancement of solid portions of the tumor admixed with nonenhancing areas of degeneration, hemorrhage, and necrosis (38,41). Enhancement is often more marked at the periphery of the tumor. Dystrophic calcification is an uncommon finding (38). At MR imaging, no specific findings distinguish retroperitoneal leiomyosarcoma. The tumor is most often iso- to hypointense relative to skeletal muscle on T1-weighted MR images, heterogeneously hyperintense on T2-weighted MR images, and heterogeneously enhancing after intravenous contrast material administration (Fig 7) (42). Although both CT and MR imaging demonstrate no specific imaging features for retroperitoneal leiomyosarcoma,

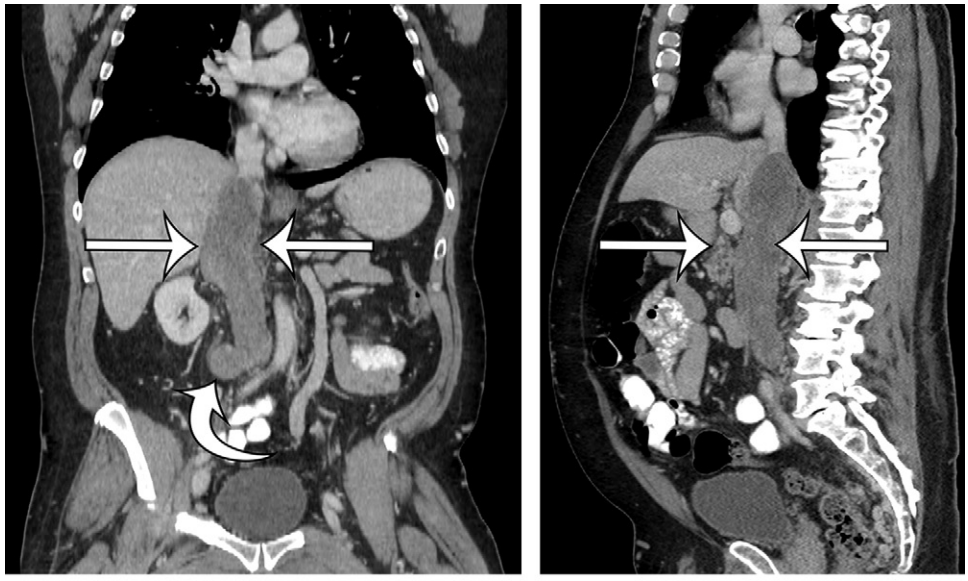

a. b.

Figure 8. Intraluminal and extraluminal leiomyosarcoma in the IVC of a 46-year-old man who presented with a 5-month history of progressive leg swelling. Coronal **(a)** and sagittal **(b)** contrast-enhanced CT images show a heterogeneously enhancing mass expanding the IVC (straight arrows), with a small round extraluminal component inferiorly (curved arrow on **a**).

it is important to recognize that leiomyosarcoma does not contain fatty elements.

Leiomyosarcomas arising from the IVC and major veins of the retroperitoneum and pelvis may manifest as an intraluminal mass (Fig 8), an extraluminal mass, or both. Leiomyosarcomas of the IVC may arise from any portion of the IVC. The attenuation characteristics at CT and the signal intensity at MR imaging are identical to those of leiomyosarcomas arising in the retroperitoneal soft tissues (Fig 9) (42). When there is an intraluminal component, the vessel is expanded by heterogeneously enhancing intraluminal tumor.

Leiomyosarcomas arising in the abdominal wall muscles tend to be smaller at the time of diagnosis, compared with retroperitoneal and IVC leiomyosarcomas. Consequently, leiomyosarcomas in the abdominal wall muscles usually demonstrate homogeneous attenuation at CT and homogeneous signal intensity at MR imaging, lacking necrosis and hemorrhage (Fig 10) (43). However, larger lesions may show heterogeneity (Fig 10) (43). Leiomyosarcomas originating in the peritoneal cavity are extremely rare. In case reports in the literature and in our experience, their imaging features are similar to those of leiomyosarcomas arising in the retroperitoneum (Fig 11) (44).

Recurrent and Metastatic Disease.—The most important prognostic factors for leiomyosarcoma are size and location. Retroperitoneal and IVC leiomyosarcomas have a high recurrence rate and are ultimately fatal because of the difficulty in achieving a curative resection. In the series of cases reported by Cooley et al (42), the most frequent sites of hematogenous metastasis were the lungs, peritoneum, and liver, followed by muscle, bones, and lymph nodes.

Gastrointestinal Stromal Tumor

Definition.—GISTs are generally defined as KIT-positive, usually *KIT* or *PDGFRA* mutation–driven mesenchymal neoplasms. They are considered to be the neoplastic equivalent of the interstitial cells of Cajal or their precursors (45).

Clinical and Pathologic Features.—GISTs are the most common mesenchymal neoplasms of the gastrointestinal tract. The biologic behavior of GISTs ranges from benign indolent lesions to highly aggressive malignancies. Malignant GISTs are the most common intraperitoneal sarcomas, and these tumors also occur in the retroperitoneum, given the retroperitoneal location of parts of the gastrointestinal tract. GISTs are most commonly found in older adults who are more than 50 years of age and only rarely occur in children. There is no race or gender predilection. GISTs in adults are typically sporadically occurring and are associated with somatic mutations in the *KIT* or *PDGFRA* gene. However, 10%–15% of GISTs lack *KIT* or *PDGFRA* mutations. These GISTs can be associated with neurofibromatosis type 1 (mainly occurring in the small intestine) or

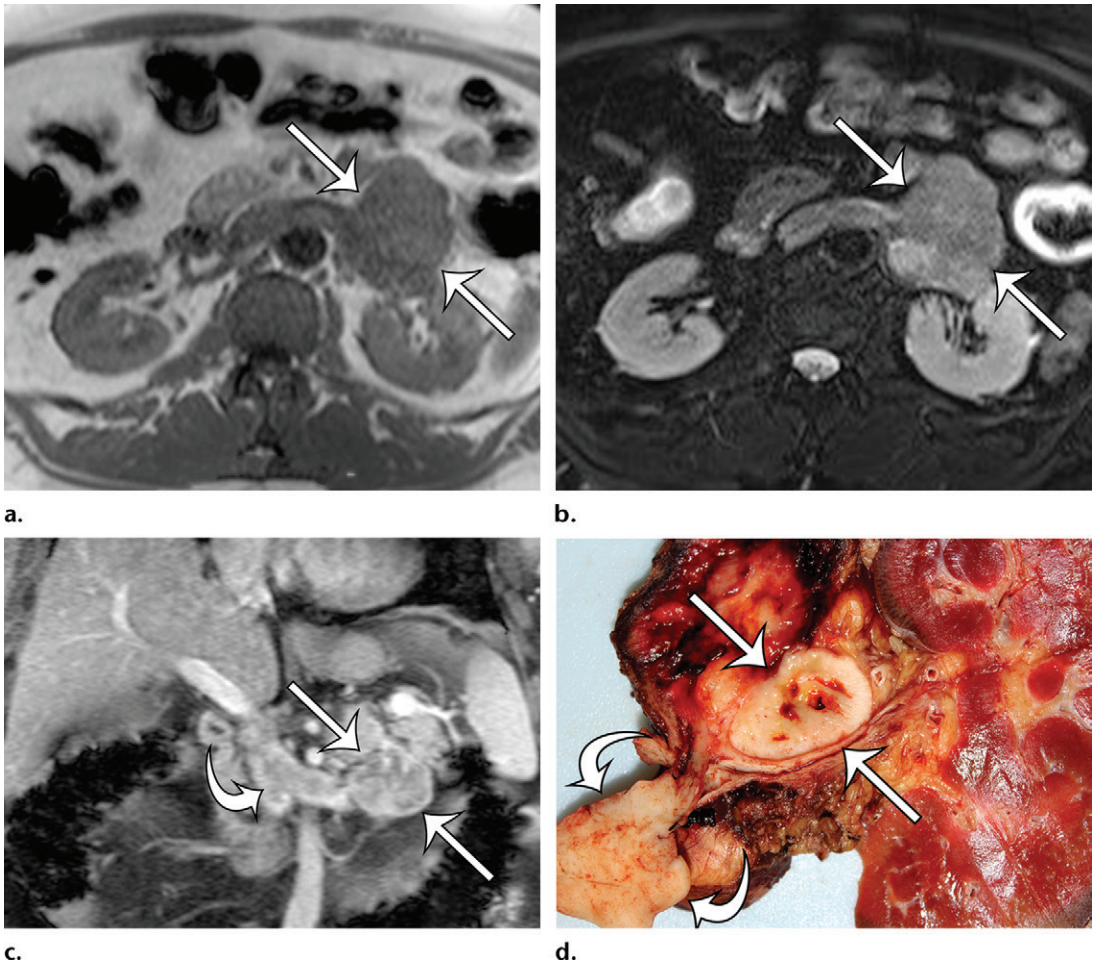

Figure 9. Leiomyosarcoma arising in the left renal vein in a 59-year-old man with progressive left flank pain. **(a, b)** Axial T1-weighted **(a)** and T2-weighted **(b)** MR images show a homogeneous mass intimately associated with the left renal vein, with an extraluminal component that is isointense to skeletal muscle on T1-weighted images (arrows on **a**) and mildly hyperintense to skeletal muscle on T2-weighted images (arrows on **b**). **(c)** Coronal gadolinium-enhanced T1-weighted fat-suppressed MR image shows enhancement of the central vein component (straight arrows) and the intraluminal tumor extending into the infrahepatic IVC (curved arrow). **(d)** Photograph of the gross specimen shows the intraluminal component adherent to the wall of the left renal vein (straight arrows) and the contiguous smooth gray-tan tumor thrombus extending beyond the resected renal vein margin (curved arrows); the tumor thrombus was milked from the IVC.

can represent succinate dehydrogenase (SDH)–deficient GISTs (mainly arising in the stomach) that include GIST in the Carney triad and the Carney-Stratakis syndrome (46,47). These tumors can be diagnosed by loss of *SDHB* gene expression in the tumor cells (48).

Approximately 60%–70% of GISTs arise in the stomach, followed by the duodenum and small bowel (20%–25%), the anus and rectum (5%), and the esophagus and colon (<5%) (49). GIST is the most common sarcoma in the peritoneal cavity and can also occur in the retroperitoneum, usually being metastatic from a gastric or intestinal primary tumor or arising from retroperitoneally located bowel. The clinical signs and symptoms of GIST depend on tumor location and size. Gastrointestinal bleeding is one of the most common symptoms. Other signs and symptoms include abdominal discomfort, pain, or distention; intestinal obstruction; and weight loss (50). Although small indolent GISTs may be asymptomatic and may be discovered incidentally during imaging and endoscopy performed for other reasons, highly malignant GISTs are typically large and symptomatic at the time of diagnosis.

GISTs arise in the muscularis propria layer of the stomach or intestinal wall. Small GISTs form intramural or serosal nodules. As they grow and expand, GISTs may develop intraluminal, intramural, and extraluminal components to varying degrees. The extraluminal component of a malignant GIST may be so large that it is difficult to determine the site of origin. Small intestinal GISTs tend to be predominantly extraluminal and attached to the intestine by a pedicle. At gross pathologic examination, the cut surface

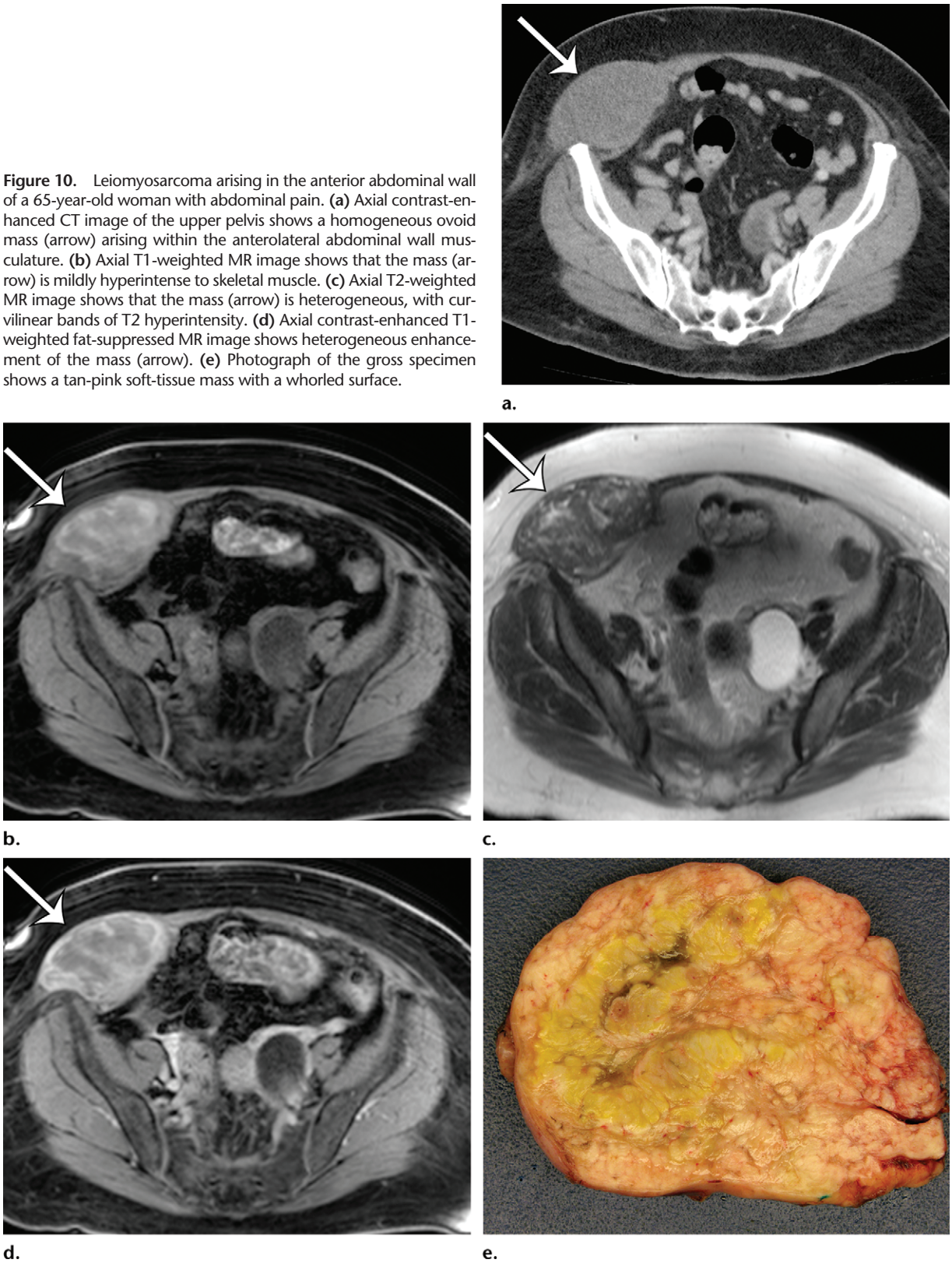

Figure 10. Leiomyosarcoma arising in the anterior abdominal wall of a 65-year-old woman with abdominal pain. **(a)** Axial contrast-enhanced CT image of the upper pelvis shows a homogeneous ovoid mass (arrow) arising within the anterolateral abdominal wall musculature. **(b)** Axial T1-weighted MR image shows that the mass (arrow) is mildly hyperintense to skeletal muscle. **(c)** Axial T2-weighted MR image shows that the mass (arrow) is heterogeneous, with curvilinear bands of T2 hyperintensity. **(d)** Axial contrast-enhanced T1-weighted fat-suppressed MR image shows heterogeneous enhancement of the mass (arrow). **(e)** Photograph of the gross specimen shows a tan-pink soft-tissue mass with a whorled surface.

of the tumor is pink, tan, or gray. Large GISTs frequently contain hemorrhage, necrosis, and cystic degeneration, which may be the predominant component. Ulceration may be present on the mucosal surface (50).

Histologically, GISTs may be cellular or hypocellular, with cells that are spindle shaped or epithelioid (Fig 12) (51). A variety of architectural patterns are seen in GISTs. The spindle-shaped cells may be arranged in fascicles similar to

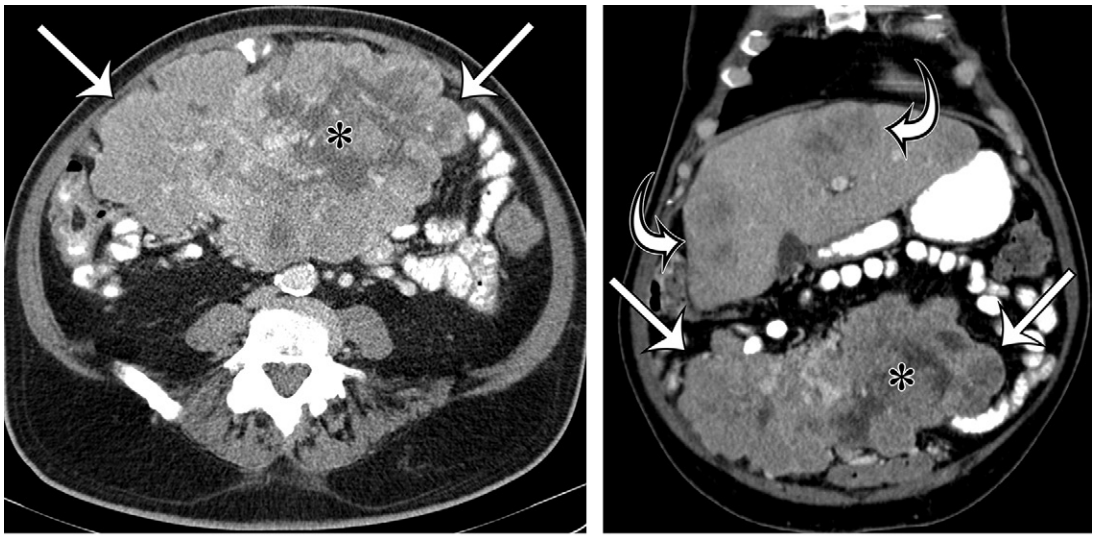

a. b.

Figure 11. Intra-abdominal leiomyosarcoma in a 75-year-old man complaining of increasing abdominal girth and abdominal pain. Axial **(a)** and coronal **(b)** contrast-enhanced CT images show a large intra-abdominal mass (straight arrows) displacing bowel loops laterally; the mass has central necrosis (*) despite prominent blood vessels. This leiomyosarcoma was metastatic at manifestation, with similar-appearing masses depicted in the liver (curved arrows on **b**).

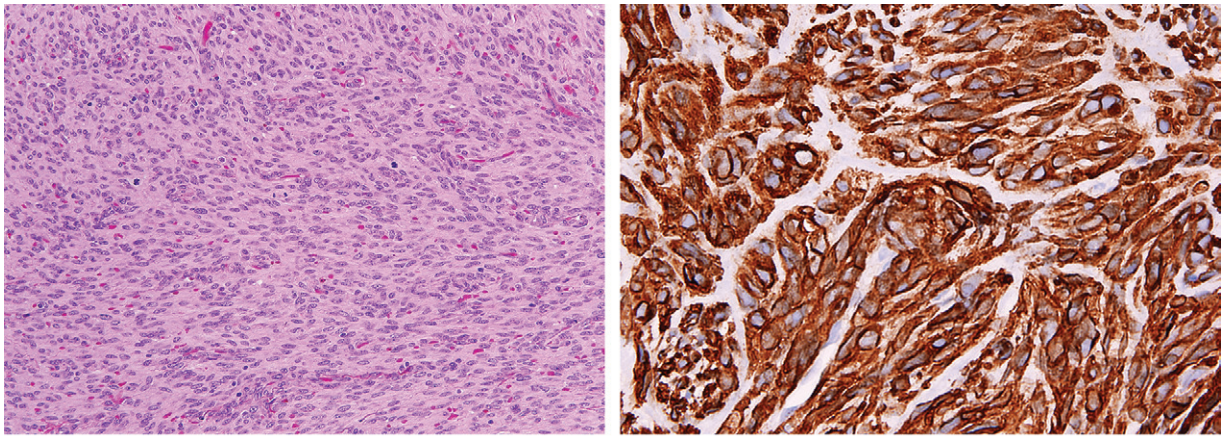

a. b.

Figure 12. Histologic features of GIST. **(a)** Photomicrograph shows that the tumor is composed of uniform spindle cells demonstrating mitotic activity. (H-E stain; original magnification, ×80.) **(b)** Photomicrograph shows that the tumor cells are strongly positive for KIT. (KIT immunohistochemical stain; original magnification, ×100.)

smooth tumors or in palisading patterns simulating neural tumors. GISTs may have prominent vascularity. The tumor stroma can be collagenous or myxoid. Extensive hyalinization and calcifications occur, especially in the smaller indolent tumors. Small intestinal GISTs may be histologically distinctive, containing extracellular collagen globules and neuropil-like material (52). Nearly all GISTs are immunohistochemically positive for KIT and DOG1/ANO1, and 70%–80% of GISTs are positive for CD34.

The prognosis of a GIST is based on the site of origin, tumor size, and mitotic rate (53–55). In general, gastric GISTs that are more than 5 cm in largest diameter and have mitotic rates of more than five mitoses per 50 high-power fields (5/50 HPFs) have a substantial risk for progressive disease. In the small bowel, tumors larger than 5 cm and even with mitotic rates of less than 5/50 HPFs have a high risk for metastatic disease.

Radiologic Features.—GISTs are well-circumscribed tumors at cross-sectional imaging. Because GISTs arise from the muscularis propria of the stomach or intestinal wall, the imaging diagnosis is based on the relationship of the mass to the wall of the gastrointestinal tract. As previously described, GISTs may be purely intramural or may have a variable intraluminal or extraluminal component (Fig 13). Intraluminal extension is most commonly seen in gastric

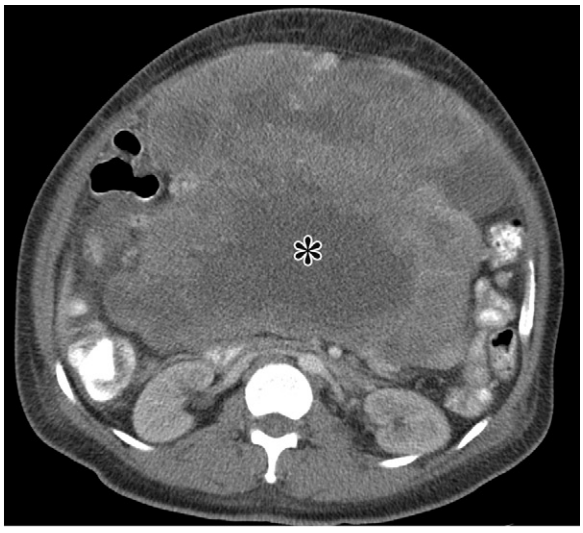

a.

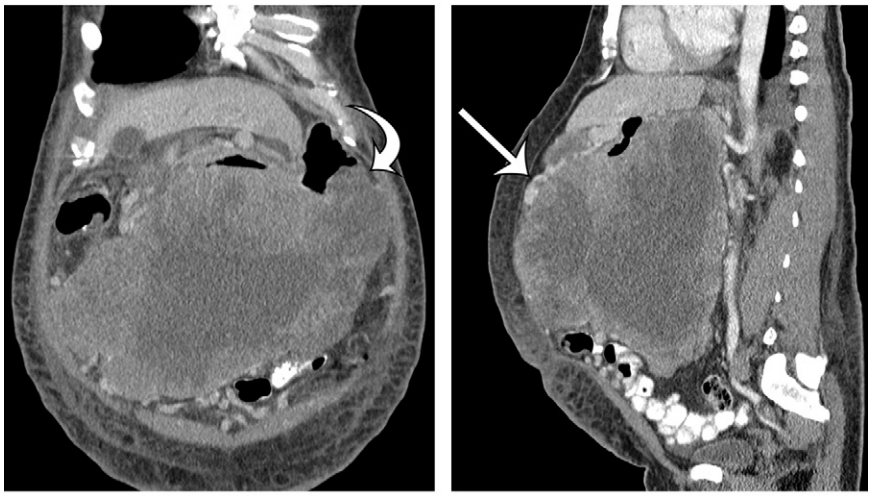

b. c.

Figure 13. GIST arising from the stomach in a 62-year-old man with abdominal distention. **(a)** Axial contrast-enhanced CT image shows a large mass with areas of low attenuation (*) in the upper abdomen. The mass compresses the superior mesenteric vein. **(b)** Coronal maximum intensity projection image shows that the mass is arising from the greater curvature of the stomach, with a polypoid intraluminal component (curved arrow). **(c)** Sagittal maximum intensity projection image shows prominent collateral vessels draped over the anterior superior tumor (arrow).

GISTs. At CT, the intraluminal component is a protrusion of tumor into the lumen of the stomach. The overlying mucosa may be smooth or may have air-filled or oral contrast material–filled defects at sites of ulceration. When an extraluminal component of the tumor is present, the tumor extends beyond the serosal surface of the gastrointestinal tract into the adjacent peritoneal cavity (50). Highly malignant GISTs may directly invade adjacent organs and tissues.

On nonenhanced CT images, GIST is usually isoattenuating to muscle. After administration of intravenous contrast material, GIST shows variable enhancement. Smaller tumors may have homogeneous enhancement. Large GISTs commonly have intratumoral degeneration, hemorrhage, and necrosis that cause a more heterogeneous pattern of enhancement (56). The degenerated, hemorrhagic, and necrotic portions of the GIST do not enhance. Necrosis and cystic degeneration may be extensive in some GISTs, such that the tumor is almost completely cystic at CT (Fig 14) (50). The presence of any residual solid enhancing tumor along the margin of the lesion and the location of the lesion arising from the wall of the gastrointestinal tract are findings that suggest that a cystic-appearing lesion may represent a GIST. Finally, calcification may be seen in GISTs at CT, and there is no distinctive pattern of calcification unique to GIST (Fig 15) (57).

The key to the imaging diagnosis of a GIST is establishing its origin from the wall of the stomach or intestine, although rare cases can appear to be extragastrointestinal (50). A minority of GISTs are described as being primary to the omentum, peritoneal cavity, or retroperitoneum, with no apparent attachment to the intestine. In the series of cases reported by Kim et al (58), omental GISTs were large in size, ranging from 10 to 27 cm in maximal diameter. Omental GISTs have well-defined borders and have extensive low-attenuation necrosis and degeneration at CT. In theory, it is possible that some

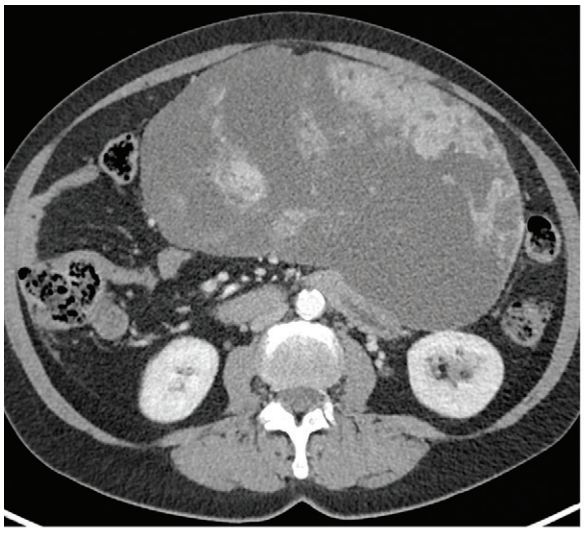

a.

b.

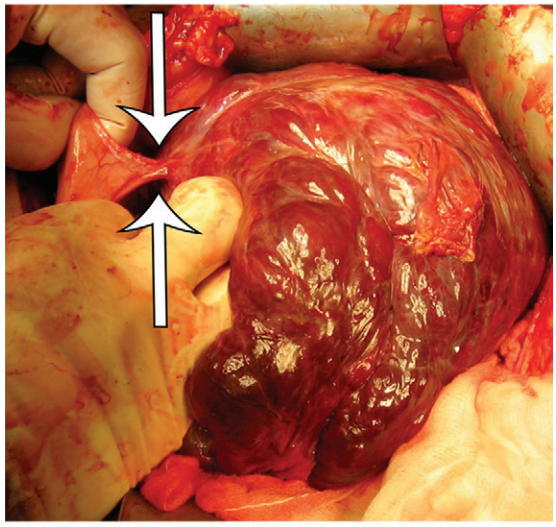

c.

Figure 14. GIST arising from the stomach in a 62-year-old woman who had pain when lying in the prone position, early satiety, and a palpable abdominal mass. **(a)** Axial contrast-enhanced CT image shows a large predominantly low-attenuation (cystic-appearing) mass within the upper abdomen. **(b)** Coronal maximum intensity projection image shows that the mass is inseparable from the greater curvature of the stomach (arrows) but is without a distinct intramural or intraluminal component. **(c)** Intraoperative photograph shows that the large lobulated well-defined mass is attached to the stomach with a thin strand of tissue (arrows).

of these GISTs originally had a narrow pedicle of attachment to the small intestine that became devascularized, allowing detachment of the GIST from the intestine.

Recurrent and Metastatic Disease.—Metastatic disease in patients with GISTs occurs most commonly in the liver and peritoneal cavity (56). Metastasis to the lung, bone, brain, and the skin and peripheral soft tissue may be seen but generally occurs late in the course of widespread metastatic disease. Although GIST with *KIT* or *PDGFRA* mutation does not metastasize to lymph nodes, succinate dehydrogenase–deficient GIST commonly metastasizes to lymph nodes, as well as the liver and peritoneal cavity (59).

Differential Diagnosis

The anatomic location and the CT attenuation and/or MR imaging signal intensity of a soft-tissue mass in the abdomen and pelvis and abdominal wall are the most important factors to consider when establishing a radiologic differential diagnosis (Table 2). Of these factors, the finding of fat within the lesion is most important because liposarcoma is the most common retroperitoneal sarcoma, and establishing fat within a lesion suspected of being liposarcoma may be diagnostic. Other fat-containing masses that may mimic well-differentiated liposarcoma include angiomyolipoma, myelolipoma, lipomatosis, and, rarely, mature lipoma. Angiomyolipomas are in the perivascular epithelioid cell tumor (also called

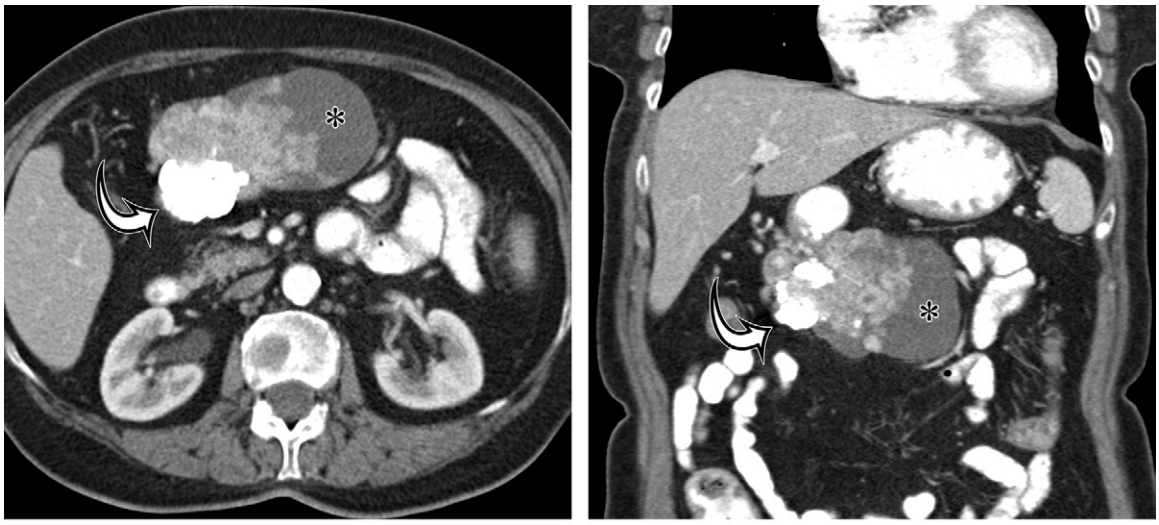

a. b.

Figure 15. GIST arising from the gastric antrum in an asymptomatic 74-year-old woman. Axial **(a)** and coronal **(b)** contrast-enhanced CT images show a mixed-attenuation mass with areas of low attenuation (*) and extensive high-attenuation calcification (curved arrow) extending along the omentum.

"PEComa") family, and most of them are benign, arising from the kidney. A large exophytic renal angiomyolipoma can be difficult to distinguish from a well-differentiated liposarcoma. The finding of a sharp defect or cleft in the renal parenchyma is characteristic of angiomyolipoma (Fig 16) (60). Other findings typical of angiomyolipoma include encapsulation, additional angiomyolipomas in the ipsilateral or contralateral kidney, associated intratumoral hemorrhage, and large vessels within the tumor. Well-differentiated liposarcoma does not invade the renal capsule because it is not an aggressive tumor. Well-differentiated liposarcoma is also hypovascular. On the other hand, dedifferentiated liposarcoma may have much more aggressive features, showing solid and enhancing elements that distinguish it from well-differentiated liposarcoma.

Myelolipoma most commonly arises from the adrenal gland and, as such, can be distinguished by an adrenal origin. True lipomas are so rare in the retroperitoneum and peritoneal cavity that the diagnosis should be made with caution and only after extensive sampling of a lipomatous mass. Excess deposition of mature fat throughout the retroperitoneum and/or pelvis, termed *lipomatosis*, can also have an appearance similar to well-differentiated liposarcoma. The CT and MR imaging findings of lipomatosis are symmetric distribution of fat in the retroperitoneum or pelvis, with preservation of the fascial planes (61). Retroperitoneal and pelvic organs are often symmetrically compressed by the fat deposition. The bladder may assume a teardrop or pear shape when the pelvis is involved.

Lastly, in the differential diagnosis of fat-containing lesions, omental infarction and fat necrosis may be masslike and mimic liposarcoma. Clinically, patients with omental infarction present with acute or subacute abdominal pain; and at imaging, inflammatory stranding and fluid are admixed with a fatty mass in the region of the greater omentum. If a large amount of the omentum is involved, twisting and torsion of the vasculature may be seen. Fat necrosis may occur anywhere in the body. In the abdomen and pelvis, fat necrosis may be complex, with an enhancing capsule and rimlike calcification, and may have mass effect on adjacent organs (Fig 17) (62). In most patients, a temporal relationship to prior trauma, surgery, or inflammation can be established with the onset of the lesion. Fat necrosis diminishes in size with time on follow-up images.

Soft-tissue sarcomas with a substantial cystic component, such as GISTs, can be misdiagnosed as an abscess or evolving hematoma. In these cases, great care should be taken to observe the relationship of the cystic lesion with respect to the adjacent stomach and intestine because most GISTs will have an origin from the stomach or intestine. The lack of an inflammatory reaction around a cystic lesion and the presence of an enhancing thick, irregular, or nodular wall are typical of a tumor with cystic degeneration, rather than an abscess or hematoma.

Myxoid components in soft-tissue sarcomas show low attenuation on CT images and show high signal intensity on T2-weighted MR images. These imaging findings may mimic fluid in an abscess, a resolving hematoma, a seroma, or a cystic mass such as a lymphangioma. Careful evaluation of the lesion in conjunction with the patient's presenting symptoms helps to resolve the overlapping findings in these entities. However, nonmalignant

Table 2: Summary of Anatomic, Pathologic, and CT Features of the Most Common Abdominal and Pelvic Sarcomas

Type of Sarcoma and Its Anatomic Locations	Gross Pathologic Features	CT Features
Well-differentiated liposarcoma		
Retroperitoneum, paratesticular soft tissues	Pale-yellow fatty mass; may have mucoid component and fibrous septa; solid nonlipogenic areas may represent dedifferentiated component	Fat-attenuation mass; may contain thin blood vessels, irregular septa, or minor nodularity; solid or large nodular component represents dedifferentiated or pleomorphic component; water-attenuation component represents myxoid component
Dedifferentiated liposarcoma		
Retroperitoneum	Firm white or yellow nonlipogenic mass	Heterogeneous solid soft-tissue mass; may contain fat-attenuation elements that are sharply demarcated from soft-tissue elements; may calcify or ossify
Leiomyosarcoma		
Retroperitoneum, pelvis, peritoneal cavity, abdominal wall	Low-grade tumors that are white or gray and may have a whorled appearance; high-grade tumors that may contain foci of necrosis or degeneration	Heterogeneous soft-tissue mass from degeneration, hemorrhage, or necrosis; intravenous contrast enhancement may be more marked at the tumor periphery; no fatty elements; dystrophic calcification is rare
Malignant GIST		
Peritoneal cavity, retroperitoneum	Intramural and subserosal nodules that may have an intraluminal component; may be pedunculated, with predominant extraluminal growth; friable, with hemorrhage on cut surface	Arises from the stomach or bowel wall, with an intramural, intraluminal, or exophytic component; well-defined margins; heterogeneous contrast enhancement; may have cystic components; may calcify

soft-tissue masses that contain myxoid or mucinous stroma are more difficult to differentiate from a sarcoma with myxoid components at imaging. In the mesentery and abdominal wall, desmoid tumors (also called fibromatosis) can have a myxoid or soft-tissue stroma (Fig 18) and appear similar to a soft-tissue sarcoma. Biopsy is necessary to establish the diagnosis before surgery. Lymphoma, metastatic disease to lymph nodes, and Castleman disease should be located in the distribution of lymph nodes chains, and nerve sheath tumors are typically in the paraspinal region.

Calcification is a common occurrence in abdominal and pelvic masses. In soft-tissue sarcomas, calcification and ossification are the consequence of metaplasia or osteochondromatous or chondrosarcomatous components of the tumor. Consequently, calcification can be seen in dedifferentiated liposarcoma, GIST, and pleomorphic undifferentiated sarcoma. Calcifications are also seen in common abdominal malignancies such as mucinous adenocarcinoma of ovarian, colorectal, pancreatic, or gastric origin. The classic mucinous calcification is a dot-dash pattern in a hypoattenuating mass. Treated lymphoma, metastatic carcinoid, teratomas, and sclerosing mesenteritis may also contain calcification. In these diseases, the soft-tissue component and associated findings typical of the disease are distinguishing features. Other forms of calcification (heterotopic ossification of the mesentery, encapsulating peritonitis, and foreign bodies) in the peritoneum are generally not a diagnostic consideration because they lack an associated mass that will be present in a soft-tissue sarcoma.

Special differential diagnostic considerations are given for those lesions arising in the abdominal wall. The differential diagnosis for abdominal wall lesions will be discussed in detail in part 2 of this article. In general, the differential diagnosis for soft-tissue sarcomas arising in the abdominal wall musculature includes dermatofibrosarcoma protuberans, desmoid tumor, endometriosis, and metastatic disease.

Clinical Considerations

Patients with soft-tissue sarcomas should be managed by a multidisciplinary team of surgeons, radiologists, pathologists, radiation oncologists, and medical oncologists with expertise and experience in soft-tissue sarcomas. Although surgery remains the principal therapy for soft-tissue sarcomas,

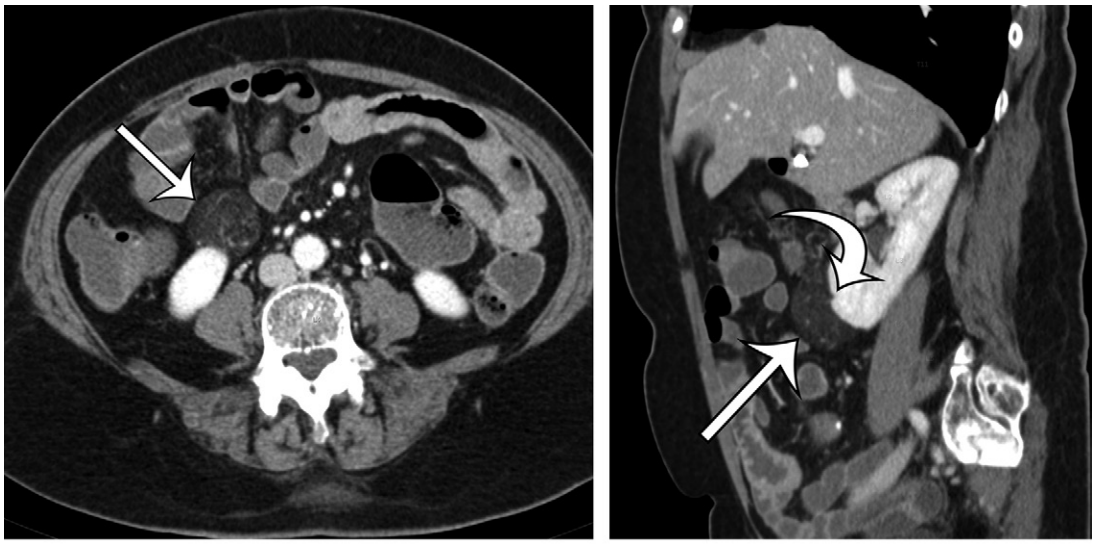

a. b.

Figure 16. Renal angiomyolipoma incidentally discovered in a 66-year-old woman at CT enterography performed for gastrointestinal bleeding. Axial **(a)** and sagittal **(b)** contrast-enhanced CT images show a well-circumscribed fat-containing lesion (straight arrow) with thin internal septa and small blood vessels. The sagittal image best shows a subtle renal cortical defect (curved arrow on **b**).

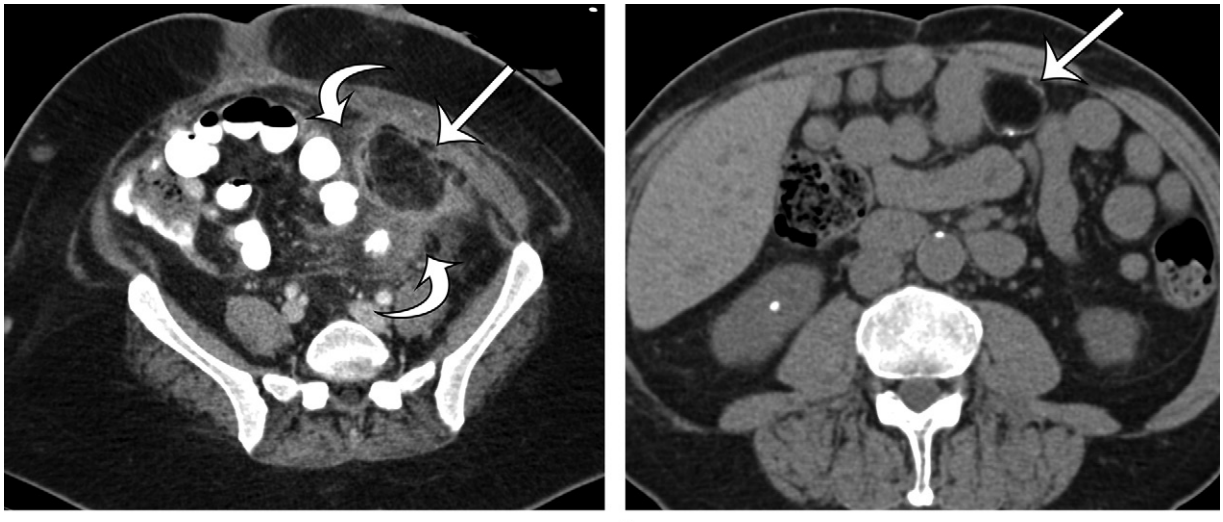

a. b.

Figure 17. Acute and chronic manifestations of fat necrosis in two patients. **(a)** Axial contrast-enhanced CT image of acute fat necrosis in a 45-year-old woman after surgery shows a partially defined fatty mass (straight arrow) in the anterior left abdomen, with substantial surrounding postoperative and inflammatory stranding and fluid (curved arrows). **(b)** Axial contrast-enhanced CT image of chronic fat necrosis in a 50-year-old man shows a well-circumscribed fatty mass (arrow) with peripheral thin calcification in the anterior left abdomen.

some tumors are not amenable to surgical resection because of the location and extent of the tumor or the presence of distant metastatic disease, or because the patient is not a surgical candidate due to comorbid conditions. The optimal resection is an R0 resection that leaves no residual microscopic disease. The resection is deemed R1 when there is residual microscopic disease and R2 when there is residual gross disease (63).

For both GIST and non-GIST sarcomas, careful evaluation of preoperative images is necessary to plan a surgical resection. For intra-abdominal, pelvic, and abdominal wall non-GIST sarcomas, the tumor location, the size, and the extent of the tumor are important because an en bloc resection of the tumor with surrounding normal tissue and organs is generally necessary to achieve microscopically negative surgical margins. Therefore, careful evaluation of the relationship of the tumor to adjacent solid viscera (commonly, the kidneys, pancreas, and spleen), bowel (most commonly, the colon), vasculature, and the abdominal wall is necessary. When the tumor arises from or involves the abdominal

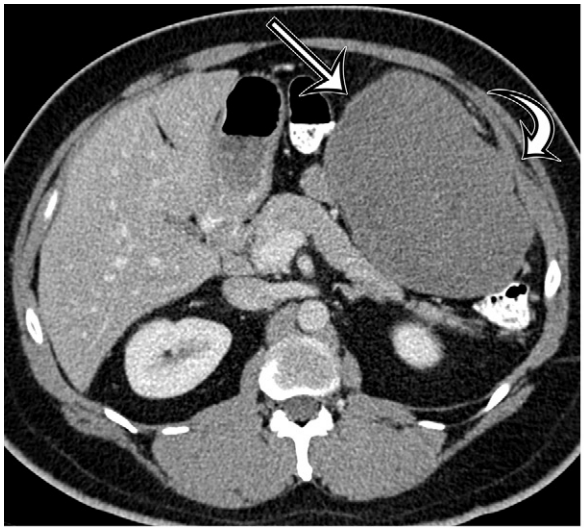

a.

b.

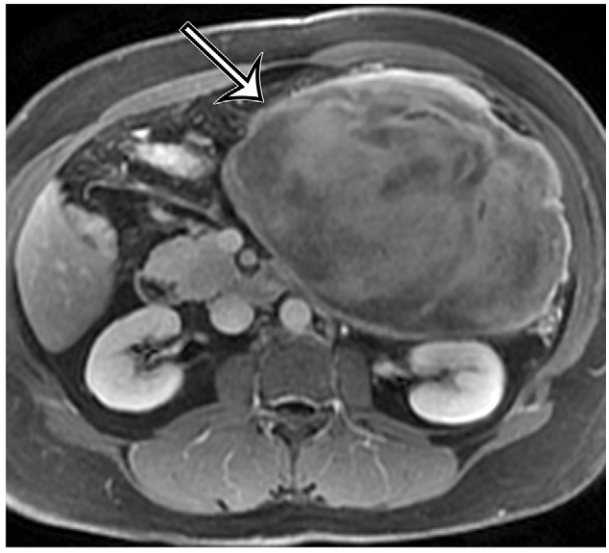

c.

Figure 18. Desmoid tumor in a 50-year-old man with vague pain in the left upper quadrant. **(a)** Axial contrast-enhanced CT image shows a well-circumscribed mass (straight arrow), which has low attenuation compared with the adherent transversus abdominis muscle (curved arrow). **(b, c)** Axial T2-weighted **(b)** and contrast-enhanced T1-weighted fat-suppressed **(c)** MR images show heterogeneous intrinsic high T2 signal intensity within the mass (arrow on **b**), with avid enhancement of the mass (arrow on **c**).

wall, reconstructive surgery may be required. In addition, multidisciplinary discussions may be needed to determine if neoadjuvant therapy would be beneficial to reduce tumor size, to increase the likelihood of an R0 resection.

For patients with GISTs, large surgical resections with wide margins are not required, because a GIST has limited intramural growth and generally no infiltrative growth. Segmental and wedge resections that can achieve microscopically negative surgical margins are performed. However, multivisceral resections may be needed in large tumors. Because a GIST is a soft and fragile tumor, great care should be taken to prevent tumor rupture and spillage, especially after preoperative tyrosine kinase therapy, because this therapy might increase tumor fragility. Neoadjuvant therapy with a tyrosine kinase inhibitor (imatinib mesylate [Gleevec]; Novartis, Basel, Switzerland) may be considered to reduce tumor size before surgery and thus achieve organ-sparing surgery.

Preoperative biopsy of non-GIST sarcomas is beneficial when the imaging characteristics of the tumor are not diagnostic of sarcoma. In general, biopsy is necessary for all masses that are not clearly liposarcoma, because the imaging features of all other soft-tissue sarcomas overlap and are not specific to a particular tumor type. Imaging-guided core needle biopsy is preferred over incisional biopsy because the former is less disruptive to tissue planes. Open surgical biopsies are strongly discouraged, because these procedures will lead to tumor rupture and increase spillage. When performing imaging-guided core needle biopsies, multiple core needle biopsy specimens (five or more) of adequate caliber (such as 18 gauge) should be obtained to have sufficient tissue not only to establish the diagnosis, but also to assess tumor grade. In our experience, sampling various locations in a large

tumor is helpful because the histologic features and grade may vary at different sites within the tumor. For those tumors suspected to be GISTs, biopsy is necessary to confirm the diagnosis for surgical planning and initiation of tyrosine kinase inhibitor therapy. Endoscopic US–guided biopsies are preferred over percutaneous biopsies, if possible, because of the potential for intraperitoneal tumor spillage with percutaneous biopsy.

Conclusion

Most abdominal and retroperitoneal sarcomas are well-differentiated or dedifferentiated liposarcomas, leiomyosarcomas, or GISTs. Many other tumor types occur with a lower frequency and will be discussed in part 2 of this article. Liposarcomas have radiologic characteristics that may allow radiology-based tumor typing. However, many other tumor types can be radiologically predicted on the basis of organ location (venous association predicts leiomyosarcoma; intestinal location predicts GIST).

References

1. Fletcher CDM, Bridge JA, Hogendoorn PCW, Mertens F, eds. WHO classification of tumours of soft tissue and bone. 4th ed. Lyon, France: IARC, 2013; 10–11.
2. Siegel RL, Miller KD, Jemal A. Cancer statistics, 2016. CA Cancer J Clin 2016;66(1):7–30.
3. Cormier JN, Pollock RE. Soft tissue sarcomas. CA Cancer J Clin 2004;54(2):94–109.
4. Baheti AD, O'Malley RB, Kim S, et al. Soft-tissue sarcomas: an update for radiologists based on the revised 2013 World Health Organization classification. AJR Am J Roentgenol 2016;206(5):924–932.
5. Gerota D. Beitrage zur kenntnis des befestigungsapparates der niere. Arch Anat Entwicklungsgesch 1895;19:265–286.
6. Zuckerkandl E. Beitrage zur anatomie des menschlichen korpers. I. Ueber den fixationsapparat der nieren. Med Jahr 1883;13(2):59–67.
7. Raptopoulos V, Kleinman PK, Marks S Jr, Snyder M, Silverman PM. Renal fascial pathway: posterior extension of pancreatic effusions within the anterior pararenal space. Radiology 1986;158(2):367–374.
8. Mindell HJ, Mastromatteo JF, Dickey KW, et al. Anatomic communications between the three retroperitoneal spaces: determination by CT-guided injections of contrast material in cadavers. AJR Am J Roentgenol 1995;164(5):1173–1178.
9. Raptopoulos V, Touliopoulos P, Lei QF, Vrachliotis TG, Marks SC Jr. Medial border of the perirenal space: CT and anatomic correlation. Radiology 1997;205(3):777–784.
10. Raptopoulos V, Lei QF, Touliopoulos P, Vrachliotis TG, Marks SC Jr. Why perirenal disease does not extend into the pelvis: the importance of closure of the cone of the renal fasciae. AJR Am J Roentgenol 1995;164(5):1179–1184.
11. Coindre JM. Grading of soft tissue sarcomas: review and update. Arch Pathol Lab Med 2006;130(10):1448–1453.
12. Edge SB, Byrd DB, Compton CC, Fritz AG, Greene FL, Trotti A, eds. AJCC cancer staging manual. 7th ed. New York, NY: Springer, 2010.
13. Pisters PW. Clinical evaluation and treatment of soft tissue tumors. In: Goldblum JR, Folpe AL, Weiss SW, eds. Enzinger and Weiss's soft tissue tumors. 6th ed. Philadelphia, Pa: Saunders/Elsevier, 2013; 11–24.
14. Enneking WF, Spanier SS, Goodman MA. A system for the surgical staging of musculoskeletal sarcoma. Clin Orthop Relat Res 1980;153:106–120.
15. Enneking WF, Spanier SS, Goodman MA. A system for the surgical staging of musculoskeletal sarcoma: 1980. Clin Orthop Relat Res 2003;415:4–18.
16. Goldblum JR, Folpe AL, Weiss SW. Liposarcoma. In: Goldblum JR, Folpe AL, Weiss SW, eds. Enzinger and Weiss's soft tissue tumors. 6th ed. Philadelphia, Pa: Saunders/Elsevier, 2013; 484–523.
17. Enzinger FM, Winslow DJ. Liposarcoma: a study of 103 cases. Virchows Arch Pathol Anat Physiol Klin Med 1962;335:367–388.
18. Dei Tos AP, Pedeutour F. Atypical lipomatous tumor. In: Fletcher CDM, Bridge JA, Hogendoorn PCW, Mertens F, eds. WHO classification of tumours of soft tissue and bone. 4th ed. Lyon, France: IARC, 2013; 33–36.
19. Weiss SW. Lipomatous tumors. Monogr Pathol 1996;38: 207–239.
20. Lucas DR, Nascimento AG, Sanjay BK, Rock MG. Well-differentiated liposarcoma: the Mayo Clinic experience with 58 cases. Am J Clin Pathol 1994;102(5):677–683.
21. Dei Tos AP. Liposarcoma: new entities and evolving concepts. Ann Diagn Pathol 2000;4(4):252–266.
22. Henricks WH, Chu YC, Goldblum JR, Weiss SW. Dedifferentiated liposarcoma: a clinicopathological analysis of 155 cases with a proposal for an expanded definition of dedifferentiation. Am J Surg Pathol 1997;21(3): 271–281.
23. Huang HY, Brennan MF, Singer S, Antonescu CR. Distant metastasis in retroperitoneal dedifferentiated liposarcoma is rare and rapidly fatal: a clinicopathological study with emphasis on the low-grade myxofibrosarcoma-like pattern as an early sign of dedifferentiation. Mod Pathol 2005;18(7):976–984.
24. Fiore M, Grosso F, Lo Vullo S, et al. Myxoid/round cell and pleomorphic liposarcomas: prognostic factors and survival in a series of patients treated at a single institution. Cancer 2007;109(12):2522–2531.
25. Kim ES, Jang SH, Park HC, Jung EH, Moon GB. Dedifferentiated liposarcoma of the retroperitoneum. Cancer Res Treat 2010;42(1):57–60.
26. Kilpatrick SE, Doyon J, Choong PF, Sim FH, Nascimento AG. The clinicopathologic spectrum of myxoid and round cell liposarcoma: a study of 95 cases. Cancer 1996;77(8): 1450–1458.
27. Azumi N, Curtis J, Kempson RL, Hendrickson MR. Atypical and malignant neoplasms showing lipomatous differentiation: a study of 111 cases. Am J Surg Pathol 1987;11(3):161–183.
28. Gebhard S, Coindre JM, Michels JJ, et al. Pleomorphic liposarcoma: clinicopathologic, immunohistochemical, and follow-up analysis of 63 cases—a study from the French Federation of Cancer Centers Sarcoma Group. Am J Surg Pathol 2002;26(5):601–616.
29. Song T, Shen J, Liang BL, Mai WW, Li Y, Guo HC. Retroperitoneal liposarcoma: MR characteristics and pathological correlative analysis. Abdom Imaging 2007;32(5): 668–674.
30. Murphey MD, Arcara LK, Fanburg-Smith J. Imaging of musculoskeletal liposarcoma with radiologic-pathologic correlation. RadioGraphics 2005;25(5):1371–1395.
31. Kim T, Murakami T, Oi H, et al. CT and MR imaging of abdominal liposarcoma. AJR Am J Roentgenol 1996;166(4): 829–833.
32. Bestic JM, Kransdorf MJ, White LM, et al. Sclerosing variant of well-differentiated liposarcoma: relative prevalence and spectrum of CT and MRI features. AJR Am J Roentgenol 2013;201(1):154–161.
33. Tateishi U, Hasegawa T, Beppu Y, Satake M, Moriyama N. Primary dedifferentiated liposarcoma of the retroperitoneum: prognostic significance of computed tomography and magnetic resonance imaging features. J Comput Assist Tomogr 2003;27(5):799–804.
34. Tallini G, Erlandson RA, Brennan MF, Woodruff JM. Divergent myosarcomatous differentiation in retroperitoneal liposarcoma. Am J Surg Pathol 1993;17(6):546–556.
35. Kim EY, Kim SJ, Choi D, et al. Recurrence of retroperitoneal liposarcoma: imaging findings and growth rates at follow-up CT. AJR Am J Roentgenol 2008;191(6):1841–1846.
36. Ghadimi MP, Al-Zaid T, Madewell J, et al. Diagnosis, management, and outcome of patients with dedifferentiated liposarcoma systemic metastasis. Ann Surg Oncol 2011;18 (13):3762–3770.

37. Lazar A, Evans HL, Shipley J. Leiomyosarcoma. In: Fletcher CDM, Bridge JA, Hogendoorn PCW, Mertens F, eds. WHO classification of tumours of soft tissue and bone. 4th ed. Lyon, France: IARC, 2013; 111–113.
38. Hartman DS, Hayes WS, Choyke PL, Tibbetts GP. Leiomyosarcoma of the retroperitoneum and inferior vena cava: radiologic-pathologic correlation. RadioGraphics 1992;12 (6):1203–1220.
39. Rajani B, Smith TA, Reith JD, Goldblum JR. Retroperitoneal leiomyosarcomas unassociated with the gastrointestinal tract: a clinicopathologic analysis of 17 cases. Mod Pathol 1999;12(1):21–28.
40. Kempson RL, Fletcher CDM, Evans HL, Hendrickson MR, Sibley RK. Atlas of tumor pathology: tumors of the soft tissues. Washington, DC: Armed Forces Institute of Pathology, 2001.
41. Lane RH, Stephens DH, Reiman HM. Primary retroperitoneal neoplasms: CT findings in 90 cases with clinical and pathologic correlation. AJR Am J Roentgenol 1989;152(1):83–89.
42. Cooley CL, Jagannathan JP, Kurra V, et al. Imaging features and metastatic pattern of non-IVC retroperitoneal leiomyosarcomas: are they different from IVC leiomyosarcomas? J Comput Assist Tomogr 2014;38(5):687–692.
43. O'Sullivan PJ, Harris AC, Munk PL. Radiological imaging features of non-uterine leiomyosarcoma. Br J Radiol 2008;81(961):73–81.
44. Bharti JN, Dey B, Desai P, Gupta R, Khurana N, Gandhi G. Primary leiomyosarcoma of peritoneal cavity. Rare Tumors 2014;6(1):5165. doi:10.4081/rt.2014.5165. Published online March 26, 2014.
45. Kindblom LG, Remotti HE, Aldenborg F, Meis-Kindblom JM. Gastrointestinal pacemaker cell tumor (GIPACT): gastrointestinal stromal tumors show phenotypic characteristics of the interstitial cells of Cajal. Am J Pathol 1998;152(5): 1259–1269.
46. Ricci R. Syndromic gastrointestinal stromal tumors. Hered Cancer Clin Pract 2016;14:15. doi:10.1186/s13053-016-0055-4. Published online July 19, 2016.
47. Stratakis CA, Carney JA. The triad of paragangliomas, gastric stromal tumours and pulmonary chondromas (Carney triad), and the dyad of paragangliomas and gastric stromal sarcomas (Carney-Stratakis syndrome): molecular genetics and clinical implications. J Intern Med 2009;266(1):43–52.
48. Miettinen M, Wang ZF, Sarlomo-Rikala M, Osuch C, Rutkowski P, Lasota J. Succinate dehydrogenase-deficient GISTs: a clinicopathologic, immunohistochemical, and molecular genetic study of 66 gastric GISTs with predilection to young age. Am J Surg Pathol 2011;35(11):1712–1721.
49. Miettinen M, Lasota J. Gastrointestinal stromal tumors: definition, clinical, histological, immunohistochemical, and molecular genetic features and differential diagnosis. Virchows Arch 2001;438(1):1–12.
50. Levy AD, Remotti HE, Thompson WM, Sobin LH, Miettinen M. Gastrointestinal stromal tumors: radiologic features with pathologic correlation. RadioGraphics 2003;23 (2):283–304.
51. Miettinen M, Sarlomo-Rikala M, Lasota J. Gastrointestinal stromal tumors: recent advances in understanding of their biology. Hum Pathol 1999;30(10):1213–1220.
52. Miettinen M, Lasota J. Histopathology of gastrointestinal stromal tumor. J Surg Oncol 2011;104(8):865–873.
53. Miettinen M, Lasota J. Gastrointestinal stromal tumors: review on morphology, molecular pathology, prognosis, and differential diagnosis. Arch Pathol Lab Med 2006;130(10): 1466–1478.
54. Miettinen M, Makhlouf H, Sobin LH, Lasota J. Gastrointestinal stromal tumors of the jejunum and ileum: a clinicopathologic, immunohistochemical, and molecular genetic study of 906 cases before imatinib with long-term follow-up. Am J Surg Pathol 2006;30(4):477–489.
55. Miettinen M, Sobin LH, Lasota J. Gastrointestinal stromal tumors of the stomach: a clinicopathologic, immunohistochemical, and molecular genetic study of 1765 cases with long-term follow-up. Am J Surg Pathol 2005;29(1): 52–68.
56. Burkill GJ, Badran M, Al-Muderis O, et al. Malignant gastrointestinal stromal tumor: distribution, imaging features, and pattern of metastatic spread. Radiology 2003;226(2): 527–532.
57. Rana R, Nikolaidis P, Miller F. Calcified gastrointestinal stromal tumor of the sigmoid colon mimicking inspissated barium on CT. AJR Am J Roentgenol 2006;187(3):W322–W323.
58. Kim HC, Lee JM, Kim SH, et al. Primary gastrointestinal stromal tumors in the omentum and mesentery: CT findings and pathologic correlations. AJR Am J Roentgenol 2004;182(6):1463–1467
59. Tirumani SH, Tirumani H, Jagannathan JP, et al. MDCT features of succinate dehydrogenase (SDH)-deficient gastrointestinal stromal tumours. Br J Radiol 2014;87(1043):20140476. http://dx.doi.org/10.1259/bjr.20140476. Published online October 13, 2014.
60. Israel GM, Bosniak MA, Slywotzky CM, Rosen RJ. CT differentiation of large exophytic renal angiomyolipomas and perirenal liposarcomas. AJR Am J Roentgenol 2002;179(3):769–773.
61. Craig WD, Fanburg-Smith JC, Henry LR, Guerrero R, Barton JH. Fat-containing lesions of the retroperitoneum: radiologic-pathologic correlation. RadioGraphics 2009;29 (1):261–290.
62. Kamaya A, Federle MP, Desser TS. Imaging manifestations of abdominal fat necrosis and its mimics. RadioGraphics 2011;31(7):2021–2034.
63. Aufforth RD, Baker JJ, Kim HJ. Soft tissue sarcoma. In: Chu QD, Gibbs JF, Zibari GB, eds. Surgical oncology: a practical and comprehensive approach. New York, NY: Springer, 2015; 605–626.